**Naval Research Laboratory**

**Washington, DC 20375-5320**

**NRL/MR/7420--14-9559**

# Investigation of Sediment Strength Characteristics in Approaches to Boston Harbor Using STING Penetrometer

ANDREI ABELEV

*Marine Physics Branch*
*Marine Geosciences Division*

September 17, 2014

# REPORT DOCUMENTATION PAGE

*Form Approved*
*OMB No. 0704-0188*



| 1. REPORT DATE *(DD-MM-YYYY)* | 2. REPORT TYPE | 3. DATES COVERED *(From - To)* |
|---|---|---|
| 17-09-2014 | Memorandum Report | |

**4. TITLE AND SUBTITLE**

Investigation of Sediment Strength Characteristics in Approaches to Boston Harbor Using STING Penetrometer

**5a. CONTRACT NUMBER**

**5b. GRANT NUMBER**

**5c. PROGRAM ELEMENT NUMBER**

**6. AUTHOR(S)**

Andrei Abelev

**5d. PROJECT NUMBER**
74-6717-A4

**5e. TASK NUMBER**

**5f. WORK UNIT NUMBER**

**7. PERFORMING ORGANIZATION NAME(S) AND ADDRESS(ES)**

Naval Research Laboratory, Code 7420
4555 Overlook Avenue, SW
Washington, DC 20375-5320

**8. PERFORMING ORGANIZATION REPORT NUMBER**

NRL/MR/7420--14-9559

**9. SPONSORING / MONITORING AGENCY NAME(S) AND ADDRESS(ES)**

Naval Research Laboratory, Code 7420
4555 Overlook Avenue, SW
Washington, DC 20375-5320

**10. SPONSOR / MONITOR'S ACRONYM(S)**

NRL

**11. SPONSOR / MONITOR'S REPORT NUMBER(S)**

**12. DISTRIBUTION / AVAILABILITY STATEMENT**

Approved for public release; distribution is unlimited.

**13. SUPPLEMENTARY NOTES**

**14. ABSTRACT**

This report discusses results of two series of STING penetrometer measurements of seafloor sediment strength in areas of Boston Harbor approach. The experimental data is analyzed and used in sediment characterization and sediment strength predictions.

**15. SUBJECT TERMS**

Seafloor strength STING
Impact burial

| 16. SECURITY CLASSIFICATION OF: | | | 17. LIMITATION OF ABSTRACT | 18. NUMBER OF PAGES | 19a. NAME OF RESPONSIBLE PERSON |
|---|---|---|---|---|---|
| a. REPORT | b. ABSTRACT | c. THIS PAGE | | | Andrei Abelev |
| Unclassified Unlimited | Unclassified Unlimited | Unclassified Unlimited | Unclassified Unlimited | 58 | 19b. TELEPHONE NUMBER *(include area code)* (202) 404-1107 |

**Standard Form 298 (Rev. 8-98)**
**Prescribed by ANSI Std. Z39.18**

# Investigation of sediment strength characteristics in approaches to Boston Harbor using STING penetrometer

## Table of Contents

## Introduction and study location

This report discusses two series of measurements of sediment bearing strength, conducted in Box 3.1nm and in Box5 – both on approach to Boston Harbor - during 01/2014 and 04/2014 trips on board Matthew Hughes (BHC). The results presented and the discussion that follows also include data from a previous trip, conducted in 12/2013 and reported earlier (*Abelev*, 2014).

The areas of sediment strength exploration included Box 3.1nmi (Fig. 1) and Box 5 (Fig. 2). Both were 1x1 nm in size. Each of the two figures includes outlines of a study box, a portion of a nautical chart, all stations where the STING measurements were performed (with station IDs), and overlays from the bottom sediment database (NAVOCEANO). Information included on the nautical chart in Box 3.1 indicates a presence of two wrecks, whereas Box 5 contains one, with only an approximate knowledge of the position. Another notable feature located just North of Box 5, is the dumping ground of dredged material. Dredged material may contain many sediment classes, typically including clay, silt, and sand, and may therefore have pronounced effects on the STING measurements; these are further discussed below. As can be seen in Fig. 2, STING measurements in Box 5 were conducted not only within the designated box limits, but also extended beyond its boundaries by approximately 500m on those sides of the box that allowed this extension. Limitations included a line of anchors to NNW of Box 5, connected to the feature, labeled "Obstruction Submerged Buoy", and the nature reserve boundary, where operations are prohibited, on the East side of the box.

The main objective in investigating these two specific locations was to find and characterize the bottom sediments that may have the lowest bearing capacity (sediment shear strength), as guided by the available sediment maps. The bulk of Box 3.1 area includes sediment labeled as Terrigenous Fine Silt, with the SE corner extending into an area of Terrigenous Silt sediment type. The survey area of Box 5 attempts to include the bulk of bottom sediments identified as Terrigenous Clay, within the limits imposed by the various obstructions and prohibited areas. Immediately adjacent to this clayey sediment is the area marked as Terrigenous Very Fine Silt. Both of these sediment types, as they appear on the available sediment map, suggest the softest conditions of the entire Boston Harbor approach area.

The coordinates of **Box 3.1**nmi were as follows:

| Field | Latitude | Longitude |
|---|---|---|
| NW Corner | 42°25.000'N | 070°39.500'W |
| NE Corner | 42°25.000'N | 070°38.150'W |
| SE Corner | 42°24.000'N | 070°38.150'W |
| SW Corner | 42°24.000'N | 070°39.500'W |

Manuscript approved July 23, 2014.

The coordinates of **Box 5** were as follows:

| Field | Latitude | Longitude |
|---|---|---|
| NW Corner | 42°23.475'N | 70°34.520'W |
| NE Corner | 42°23.700'N | 70°33.200'W |
| SE Corner | 42°22.725'N | 70°32.895'W |
| SW Corner | 42°22.500'N | 70°34.215'W |

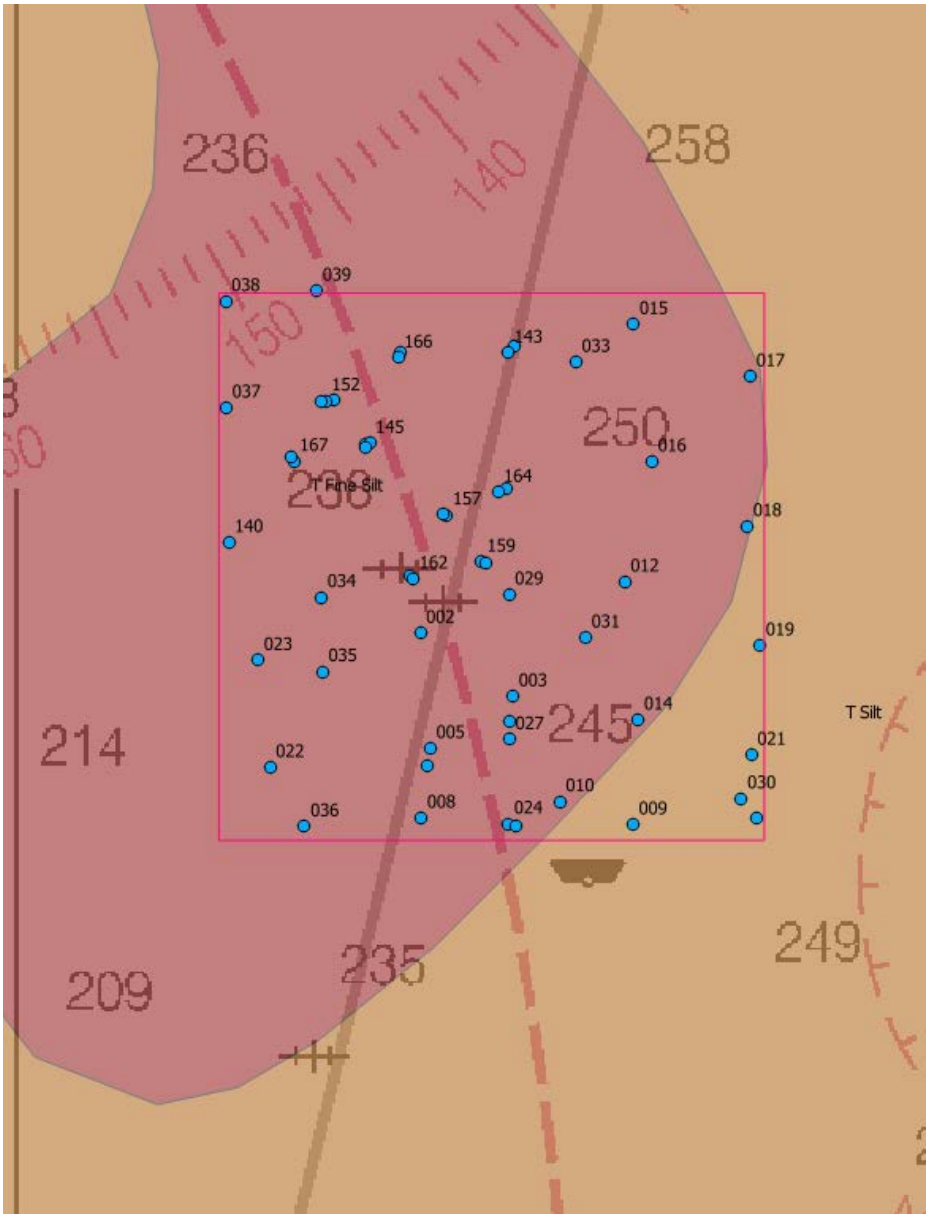


**Fig. 1 Box 3.1nmi study area (red outline); STING deployments (in blue with station numbers), nautical chart overlay and NAVOCEANO sediment map overlay – majority of Box 3.1nmi is in Terrigenous Fine Silt (purple), South-East corner is in Terrigenous Silt (brown)**

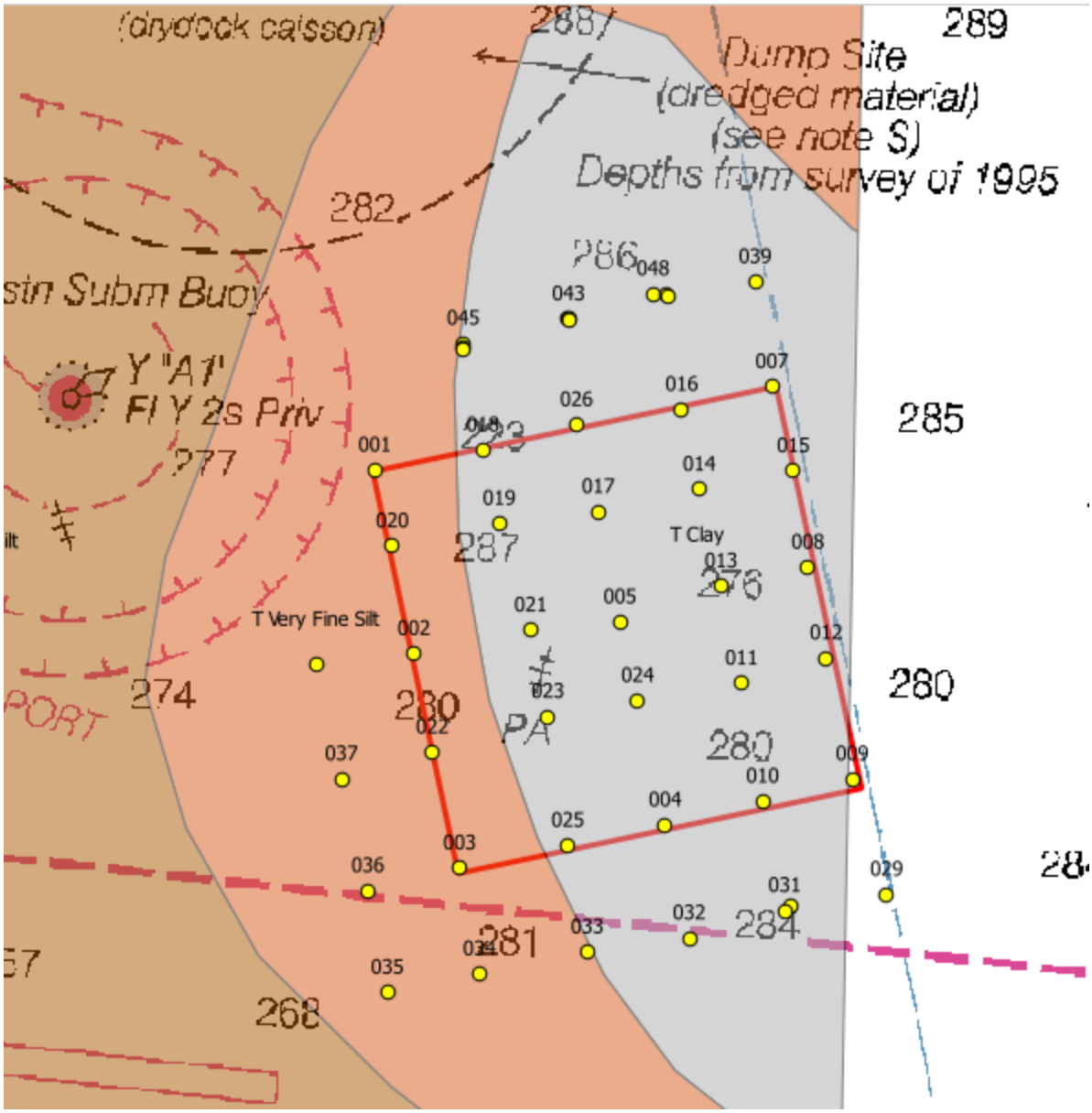


**Fig. 2 Box5 study area (red outline), STING positions (in yellow, with drop numbers), Nautical chart overlay, NAVOCEANO sediment map overlay – most of Box 5 is in Terrigenous Clay (gray), West margin is in Terrigenous Very Fine Silt (light brown)**

## Instrumentation

A set of three 7420 STINGs (Sea Terminal Impact Naval Gradiometer - *Jasco Research Ltd.*, 2002) was used in conducting sediment analysis for bearing strength. These probes consist of a fin-stabilized main body with extension/penetrator rods attached to it (Fig. 3a). Several diameter foot-plates can be attached to the bottom (penetrating) end of these extension rods, including 25, 35, 50, and 70mm diameter. The main body of the probe (Fig. 3b) includes a single axis accelerometer, water pressure transducer, and data acquisition and storage unit with the total on-board memory sufficient for 4.5 min data acquisition, when recording in dual-channel mode (acceleration and water pressure). During this time interval, repeated drops of the penetrometer are conducted at each station to provide for averaging necessary in naturally heterogeneous seafloor sediment conditions. Normally, three to four drops per location were performed.

Selection of the STING foot diameter may be guided by several considerations, including intended depth of penetration where the smaller the foot diameter, the greater is the resulting penetration burial thus maximizing the depth surveyed with the probe; the quality of data used in correlations with the sediment undrained shear strength, as some diameters may yield better modeling outcomes due to a variety of soil plastic flow effects around the penetrometer foot; or direct empirical relations between the maximum depth of the penetrating probe with expected depth of burial of larger objects. These size effects were studied with several penetrometers of varying dimensions (*Mulhearn*, 2002) and showed that little change in *maximum burial* occurs for circular bodies of diameter greater than 70 mm. During this survey, a 75mm foot was utilized, to utilize the benefits of these direct correlations.

In general, the numerical model used in retrieving the sediment strength from deceleration records of probes is applicable to cohesive materials (clays and silts) or mixtures that exhibit a mostly cohesive behavior. If thick enough layers of sandy material are present, they result in

(a) (b)

**Fig. 3 (a) STING with 2m rods and several different foot sizes attached (25mm – left, 35mm – middle, 70mm – right); (b) STING before deployment with tail cone and tether attached**

characteristic spikes in acceleration (and thus the derived bearing strength) records, due to the dilative effects in the sandy material matrix. These layers need not be clean sand to impose this effect and are most likely a mixture with surrounding finer-grained material (silt and clay). These dilative effects, however, may severely impede penetration of various objects, especially when the impact velocities are high (*e.g.* greater than 1 meter per second) relative to the overall sediment permeability or the ability to dissipate excess pore water pressures quickly. For further information on the effects of dilation on dynamic penetration, the reader is referred to *Stoll et al.*, 2007.

The range of the accelerometer used in the STINGs is chosen in such a way as to maximize resolution in investigating mostly cohesive/clayey soils. When significantly higher resistance is encountered in sandy layers, the accelerometer often saturates, exceeding the range. Part of the calculation may still be conducted, retrieving the pseudo-strength values, but these should be treated with care, as they lay outside the normal range of the sediment strength retrieval model.

Such series of spikes (leading to accelerometer saturation) were encountered in both study boxes (Figs. 4 and 5) and are especially numerous in Box 3.1. In Box 5, these effects were observed at only one station (#18). These figures (4 and 5) show the variation of the calculated shear strength with sediment depth and include all individual STING drops. These plots are useful in identifying the overall spectrum of material encountered at each location, the spread in the data and possible similarities between drops and stations.

## Results: STING penetration and shear strength

The results of the STING deployments are summarized in Table 1 for Box 5 and Table 2 for Box 3.1. Each station includes an average of typically three STING drops. Maximum penetration values are shown and include the average and the standard deviation values of all the drops performed at each station.

Examination of the burial data from Box 5 shows relatively deep penetrations, indicating soft sediment strength, with the exception of one – Station # 18, also highlighted in the table and also labeled in Fig. 5. Additionally, whereas the water depth at all locations was relatively uniform of around 91m, this one station (#18) was much shallower, at only at 81m of water depth, representing a mound that is almost 10m above the adjacent seafloor. The overall penetration burial of the probe at this station is very small – only 18cm on average. The calculated bearing strength profiles for each of the three drops at this location (Station 18, Box 5) are shown in Fig. 6, demonstrating a response of a typical dilative sandy layer that begins very close to the sediment-water interface (perhaps at 3cm mark). This location may be a result of dumping of dredged material that nominally (according to the nautical chart) should only be found about 1km north of this station.

**Table 1 STING deployment list, 03/2014 trials, Box 5, Boston Harbor approach**

| Station number | Lat, deg | Lon, deg | Date, EST | Water depth, m | Average Penetration depth, m | STDEV depth, m |
|---|---|---|---|---|---|---|
| 1 | 42.3913 | -70.57523 | 3/5/2014 | 92 | **0.65** | 0.06 |
| 2 | 42.38388 | -70.5729 | 3/5/2014 | 90 | **0.70** | 0.01 |
| 3 | 42.37521 | -70.57018 | 3/5/2014 | 90 | **0.70** | 0.04 |
| 4 | 42.37711 | -70.55897 | 3/5/2014 | 91 | **0.64** | 0.03 |
| 5 | 42.38532 | -70.56165 | 3/5/2014 | 91 | **0.70** | 0.07 |
| 7 | 42.39498 | -70.55357 | 3/5/2014 | 92 | **0.76** | 0.07 |
| 8 | 42.38768 | -70.55142 | 3/5/2014 | 91 | **0.81** | 0.05 |
| 9 | 42.37912 | -70.54878 | 3/5/2014 | 91 | **0.84** | 0.01 |
| 10 | 42.37815 | -70.55366 | 3/5/2014 | 92 | **0.75** | 0.02 |
| 11 | 42.38292 | -70.55493 | 3/5/2014 | 90 | **0.81** | 0.03 |
| 12 | 42.38401 | -70.55032 | 3/5/2014 | 91 | **0.67** | 0.02 |
| 13 | 42.38685 | -70.55615 | 3/5/2014 | 90 | **0.69** | 0.02 |
| 14 | 42.39076 | -70.55744 | 3/5/2014 | 91 | **0.75** | 0.07 |
| 15 | 42.39158 | -70.55231 | 3/5/2014 | 92 | **0.69** | 0.03 |
| 16 | 42.39399 | -70.55848 | 3/5/2014 | 93 | **0.67** | 0.01 |
| 17 | 42.38978 | -70.56295 | 3/5/2014 | 93 | **0.70** | 0.03 |
| 18 | 42.3922 | -70.56933 | 3/5/2014 | 81 | **0.14** | 0.07 |
| 19 | 42.38923 | -70.56836 | 3/5/2014 | 94 | **0.67** | 0.02 |
| 20 | 42.38823 | -70.57419 | 3/5/2014 | 92 | **0.75** | 0.11 |
| 21 | 42.38492 | -70.56653 | 3/5/2014 | 92 | **0.81** | 0.10 |
| 22 | 42.3799 | -70.57179 | 3/5/2014 | 91 | **0.69** | 0.03 |
| 23 | 42.38143 | -70.5655 | 3/5/2014 | 92 | **0.74** | 0.04 |
| 24 | 42.38214 | -70.5606 | 3/5/2014 | 92 | **0.74** | 0.03 |
| 25 | 42.37621 | -70.56428 | 3/5/2014 | 92 | **0.76** | 0.05 |
| 26 | 42.39329 | -70.56423 | 3/5/2014 | 94 | **0.78** | 0.04 |
| 29 | 42.37446 | -70.54678 | 3/5/2014 | 90 | **0.73** | 0.02 |
| 30 | 42.37393 | -70.55204 | 3/5/2014 | 90 | **0.66** | 0.06 |
| 32 | 42.37254 | -70.55754 | 3/5/2014 | 90 | **0.62** | 0.02 |
| 33 | 42.3719 | -70.56311 | 3/5/2014 | 89 | **0.66** | 0.04 |
| 34 | 42.37093 | -70.56899 | 3/5/2014 | 88 | **0.63** | 0.04 |
| 35 | 42.37011 | -70.57401 | 3/5/2014 | 87 | **0.67** | 0.02 |
| 36 | 42.37422 | -70.57518 | 3/5/2014 | 88 | **0.67** | 0.05 |
| 37 | 42.37874 | -70.57674 | 3/5/2014 | 89 | **0.61** | 0.05 |
| 38 | 42.38341 | -70.57817 | 3/5/2014 | 89 | **0.64** | 0.02 |
| 39 | 42.39923 | -70.55459 | 3/5/2014 | 92 | **0.76** | 0.04 |
| 42 | 42.39764 | -70.56482 | 3/5/2014 | 93 | **0.70** | 0.04 |
| 45 | 42.39651 | -70.57051 | 3/5/2014 | 93 | **0.63** | 0.03 |
| 48 | 42.39866 | -70.56017 | 3/5/2014 | 92 | **0.76** | 0.09 |

**Table 2 STING deployment list, 01/2014 trials, Box 3.1nmi, Boston Harbor approach[1]. All water depths were approximately 74m**

| Station number | Lat, deg | Lon, deg | Date, EST | Average penetration depth, m | STDEV penetration depth, m |
|---|---|---|---|---|---|
| 2 | 42.40631 | -70.65003 | 1/29/2014 | **0.44** | 0.01 |
| 3 | 42.40438 | -70.64621 | 1/29/2014 | **0.48** | 0.02 |
| 5 | 42.40280 | -70.64961 | 1/29/2014 | **0.32** | 0.03 |
| 6 | 42.40227 | -70.64975 | 1/29/2014 | **0.29** | 0.08 |
| 8 | 42.40068 | -70.64999 | 1/29/2014 | **0.32** | 0.02 |
| 9 | 42.40048 | -70.64126 | 1/29/2014 | **0.52** | 0.06 |
| 10 | 42.40118 | -70.64427 | 1/29/2014 | **0.51** | 0.02 |
| 12 | 42.40787 | -70.64160 | 1/29/2014 | **0.52** | 0.05 |
| 14 | 42.40367 | -70.64104 | 1/29/2014 | **0.54** | 0.03 |
| 15 | 42.41571 | -70.64123 | 1/29/2014 | **0.51** | 0.04 |
| 16 | 42.41153 | -70.64047 | 1/29/2014 | **0.53** | 0.02 |
| 17 | 42.41412 | -70.63641 | 1/29/2014 | **0.53** | 0.04 |
| 18 | 42.40956 | -70.63654 | 1/29/2014 | **0.61** | 0.06 |
| 19 | 42.40593 | -70.63602 | 1/29/2014 | **0.44** | 0.02 |
| 21 | 42.40260 | -70.63637 | 1/29/2014 | **0.50** | 0.02 |
| 22 | 42.40222 | -70.65623 | 1/29/2014 | **0.11** | 0.08 |
| 23 | 42.40548 | -70.65672 | 1/29/2014 | **0.26** | 0.04 |
| 24 | 42.40050 | -70.64640 | 1/30/2014 | **0.49** | 0.03 |
| 25 | 42.40043 | -70.64607 | 1/30/2014 | **0.45** | 0.01 |
| 26 | 42.40361 | -70.64634 | 1/30/2014 | **0.49** | 0.02 |
| 27 | 42.40307 | -70.64635 | 1/30/2014 | **0.51** | 0.03 |
| 29 | 42.40748 | -70.64637 | 1/30/2014 | **0.51** | 0.01 |
| 30 | 42.40127 | -70.63678 | 1/30/2014 | **0.51** | |
| 31 | 42.40617 | -70.64321 | 1/30/2014 | **0.55** | 0.01 |
| 32 | 42.40066 | -70.63613 | 1/30/2014 | **0.54** | 0.01 |
| 33 | 42.41456 | -70.64361 | 1/30/2014 | **0.62** | 0.00 |
| 34 | 42.40740 | -70.65410 | 1/30/2014 | **0.36** | 0.01 |
| 35 | 42.40514 | -70.65406 | 1/30/2014 | **0.34** | 0.01 |
| 36 | 42.40042 | -70.65480 | 1/30/2014 | **0.16** | 0.02 |
| 37 | 42.41317 | -70.65803 | 1/30/2014 | **0.30** | 0.01 |
| 38 | 42.41641 | -70.65806 | 1/30/2014 | **0.18** | 0.01 |
| 39 | 42.41673 | -70.65430 | 1/30/2014 | **0.47** | 0.02 |
| 140 | 42.40907 | -70.65793 | 12/4/2013 | **0.29** | 0.01 |
| 143 | 42.41484 | -70.64640 | 12/4/2013 | **0.52** | |

[1] STDEV values are omitted in cases of insufficient data (too few drops per station)

| Station number | Lat, deg | Lon, deg | Date, EST | Average penetration depth, m | STDEV penetration depth, m |
|---|---|---|---|---|---|
| 144 | 42.41205 | -70.65227 | 12/5/2013 | **0.42** | 0.02 |
| 145 | 42.41209 | -70.65211 | 12/5/2013 | **0.46** | 0.01 |
| 146 | 42.41198 | -70.65230 | 12/5/2013 | **0.35** | 0.09 |
| 151 | 42.41340 | -70.65362 | 12/5/2013 | **0.39** | 0.02 |
| 152 | 42.41338 | -70.65393 | 12/5/2013 | **0.30** | 0.04 |
| 153 | 42.41334 | -70.65411 | 12/5/2013 | **0.20** | 0.04 |
| 157 | 42.40991 | -70.64893 | 12/5/2013 | **0.54** | 0.01 |
| 158 | 42.40995 | -70.64910 | 12/5/2013 | **0.52** | 0.02 |
| 159 | 42.40848 | -70.64752 | 12/5/2013 | **0.54** | 0.03 |
| 160 | 42.40843 | -70.64730 | 12/5/2013 | **0.55** | 0.05 |
| 161 | 42.40805 | -70.65048 | 12/5/2013 | **0.33** | 0.06 |
| 162 | 42.40796 | -70.65031 | 12/5/2013 | **0.39** | 0.02 |
| 163 | 42.41071 | -70.64648 | 12/5/2013 | **0.55** | 0.03 |
| 164 | 42.41060 | -70.64683 | 12/5/2013 | **0.55** | 0.03 |
| 165 | 42.41486 | -70.65087 | 12/5/2013 | **0.47** | 0.01 |
| 166 | 42.41469 | -70.65094 | 12/5/2013 | **0.25** | 0.08 |
| 167 | 42.41154 | -70.65525 | 12/5/2013 | **0.24** | 0.05 |
| 168 | 42.41168 | -70.65537 | 12/5/2013 | **0.25** | 0.08 |

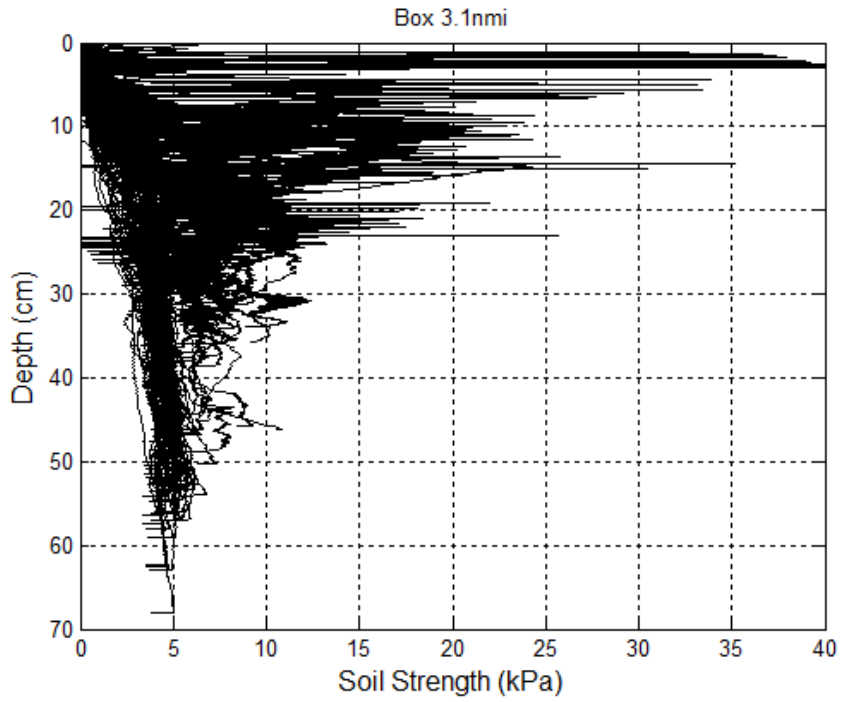


**Fig. 4 STING-derived Shear Strength values (70mm foot) vs. sediment depth. Each curve represents an individual STING drop.**

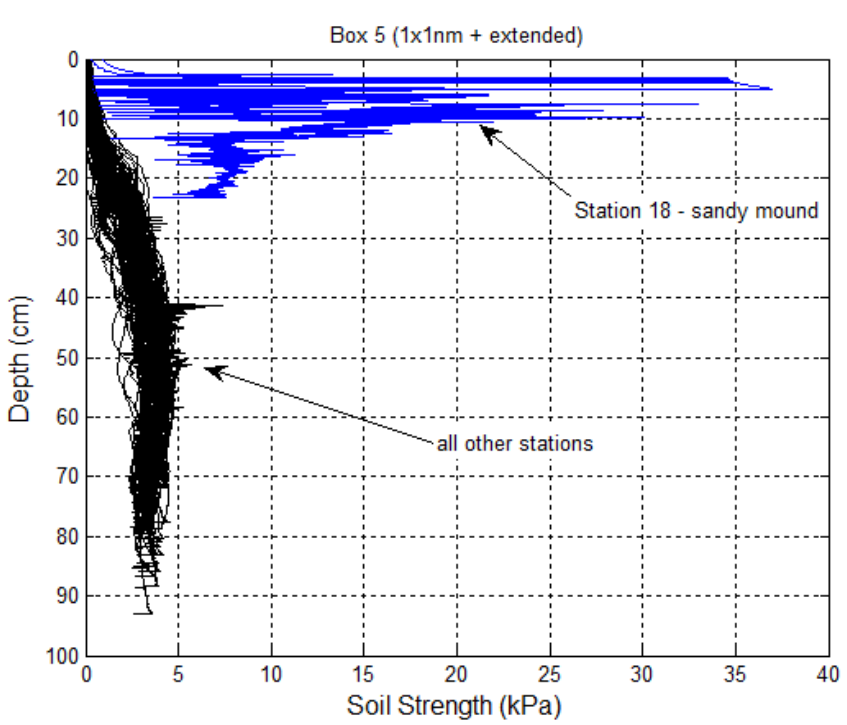


**Fig. 5 STING-derived Shear Strength values (70mm foot) vs. sediment depth. Each curve is an individual STING drop. Three drops at station 18 (blue) are shown as being distinctly different from the rest of the ensemble (black). Overall uniformity over the entire are is high, describing a soft clayey sediment type**

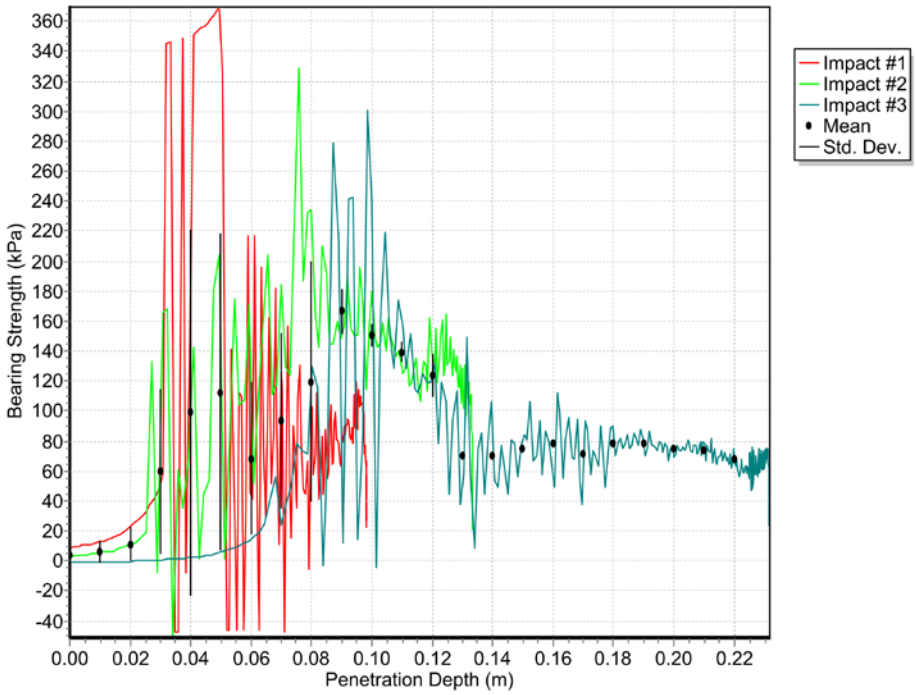


**Fig. 6 Bearing strength profile at Station #18, Box 5 (STING: 2m rod, 70mm foot, water depth: 81m)**

The exact extend of this mound, based on the STING results alone, is less than the spacing between the stations (or less than 500m), since all of the adjacent test sites demonstrate normal response, characteristic of the soft clayey material of the area in Box 5, with no discernable presence of sandy layers at the surface or in depth. If overlaying the STING deployment stations with data available from Google Earth™, the mound is apparent (Fig. 7), confirming the deposition of a foreign (to this area) likely dredged material that appears to be mostly sand. Presence of sand at about 3cm in depth with some soft material over the top, as well as a developed seafloor settlement on the perimeter of the mound, also visible in the figure, indicates that this is not a recent deposition. Considering 0.3cm/yr approximate soft sediment deposition rates in this area (*Alperin et al.*, 2002; *Crusius et al.*, 2004), one may estimate that the dump occurred approximately 10 years ago.

Examination of all the penetration histories (see Appendix A) indicates that no sandy layers of any significant extent were detected at the other stations in Box 5, except for station 18. Some such spikes and oscillations in the acceleration (and therefore bearing strength) record are only occasionally present at several stations in Box 5, other than Station 18, with perhaps, only one drop out of typical three per station, exhibiting this response. These are best attributed to a sudden deceleration of the probe when hitting a single shell or a similarly-sized marine organism or other obstruction in the sediment. If not repeated in all drops on that station or in the same area, such a single event is an unlikely indicator of sandy layer (or lens) of any significant extent.

Fig. 8 shows the values of maximum penetration burial of the 70mm STINGs in Box 5 as well as the surrounding area explored. Most of the box shows relatively even distribution of burial values, indicating essentially similar sediment with exception of the northern portion, discussed above.

The results of the STING burial in Box 3.1 are given in Fig. 9, with both nautical chart and sediment class overlays. The sediment appears to be quite variable, with one station yielding a penetration burial of over 60cm whereas another of only 11cm. As is also evident from Fig. 4, most stations contain significant presence of sandy layers, resulting in high dilation values and overall low penetration. The details of all the bearing strength measurements for this location are also given in Appendix B, showing the prevalence of the oscillatory behavior caused by these dilative effects.

While attempting to classify the sediment in Box 3.1 according to the maximum STING burial values, also indicative of burial of much larger bodies, as discussed above, a contour map was computed from the point data. While sparse, resulting in some contour irregularities, it is nonetheless notable in identifying a portion of Box 3.1 with softest material. Similar contour plotting for Box 5 was found to be not informative due to the overall similarity of the material, with the exception of the bottom mound feature.


**Fig. 7 STING positions with an overlaid bathymetric image (Google DigitalGlobe™, 2004), showing the abnormality near the NW corner of Box 5 – a mound that may have resulted from dredged material dumping**

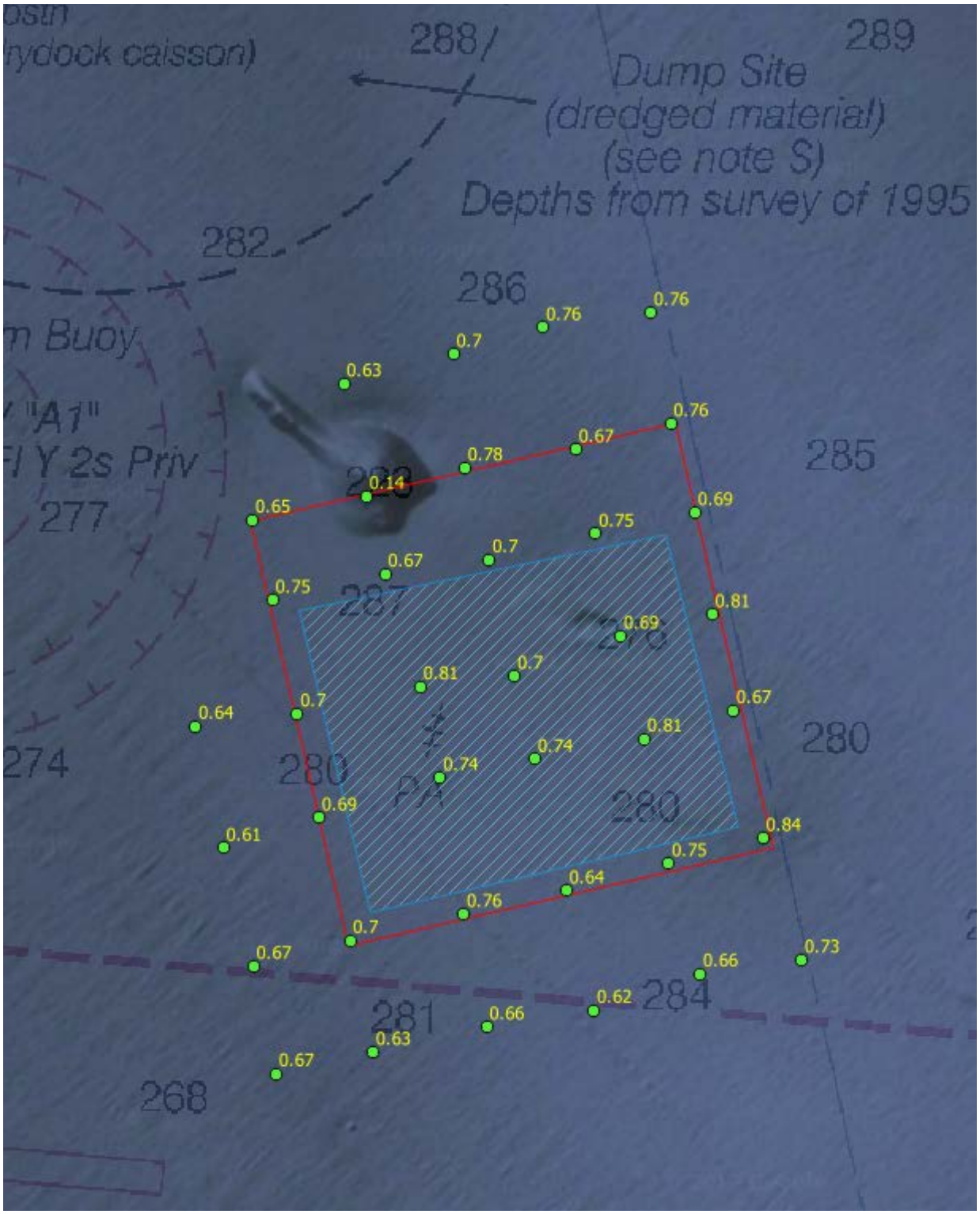


**Fig. 8 Maximum burial depths (STINGs 70mm, each value – an average of three drops), with bathymetry (Google DigitalGLobe™) and Nautical Chart overlays, and a selected area of potential impact burial of at least 70cm**

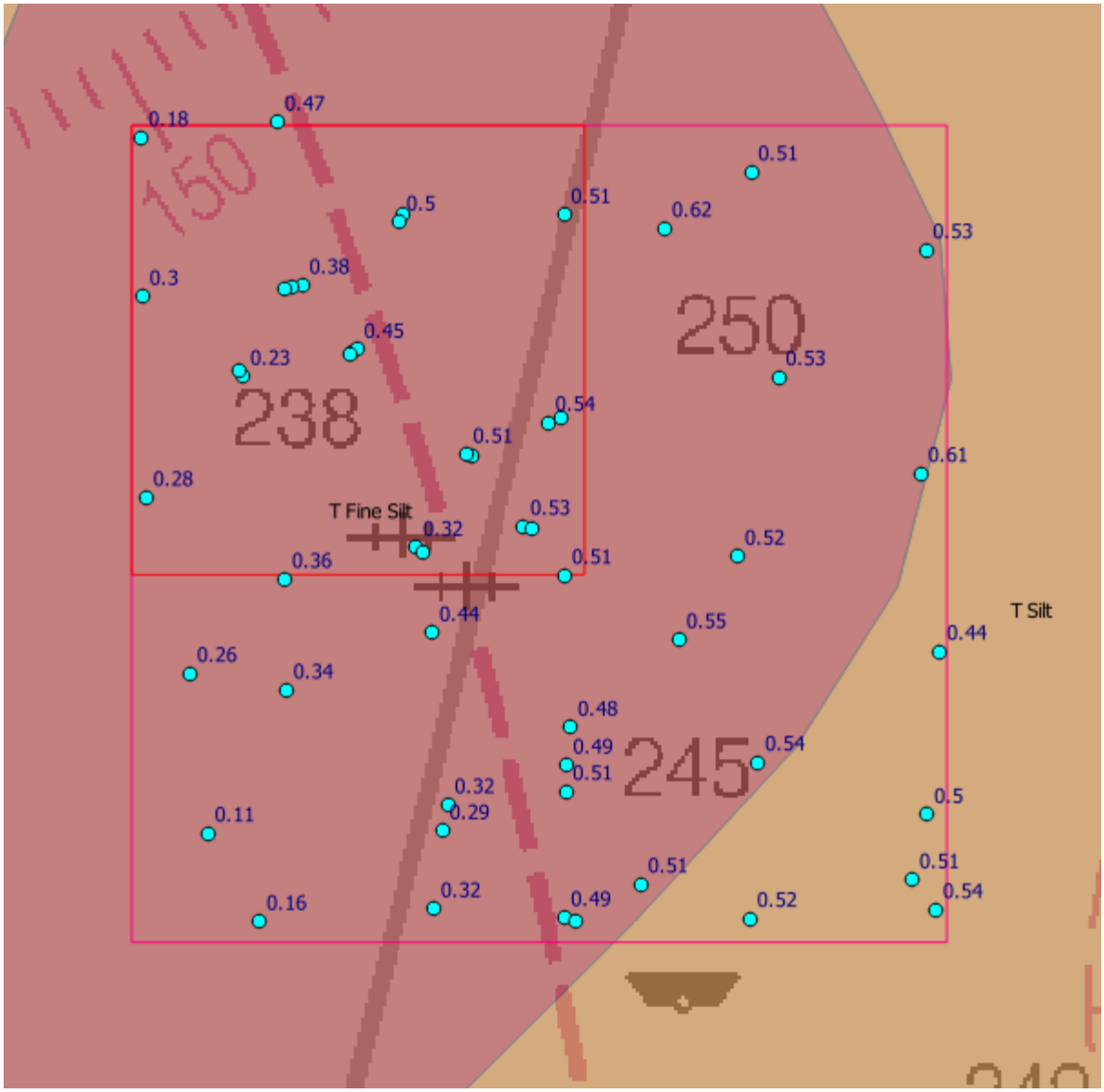


**Fig. 9 Maximum burial depths (STINGs 70mm, averages of several drops, in meters), with the Nautical Chart overlay. Larger area is Box 3.1nmi, small area inside it (NW part) is Box 3**

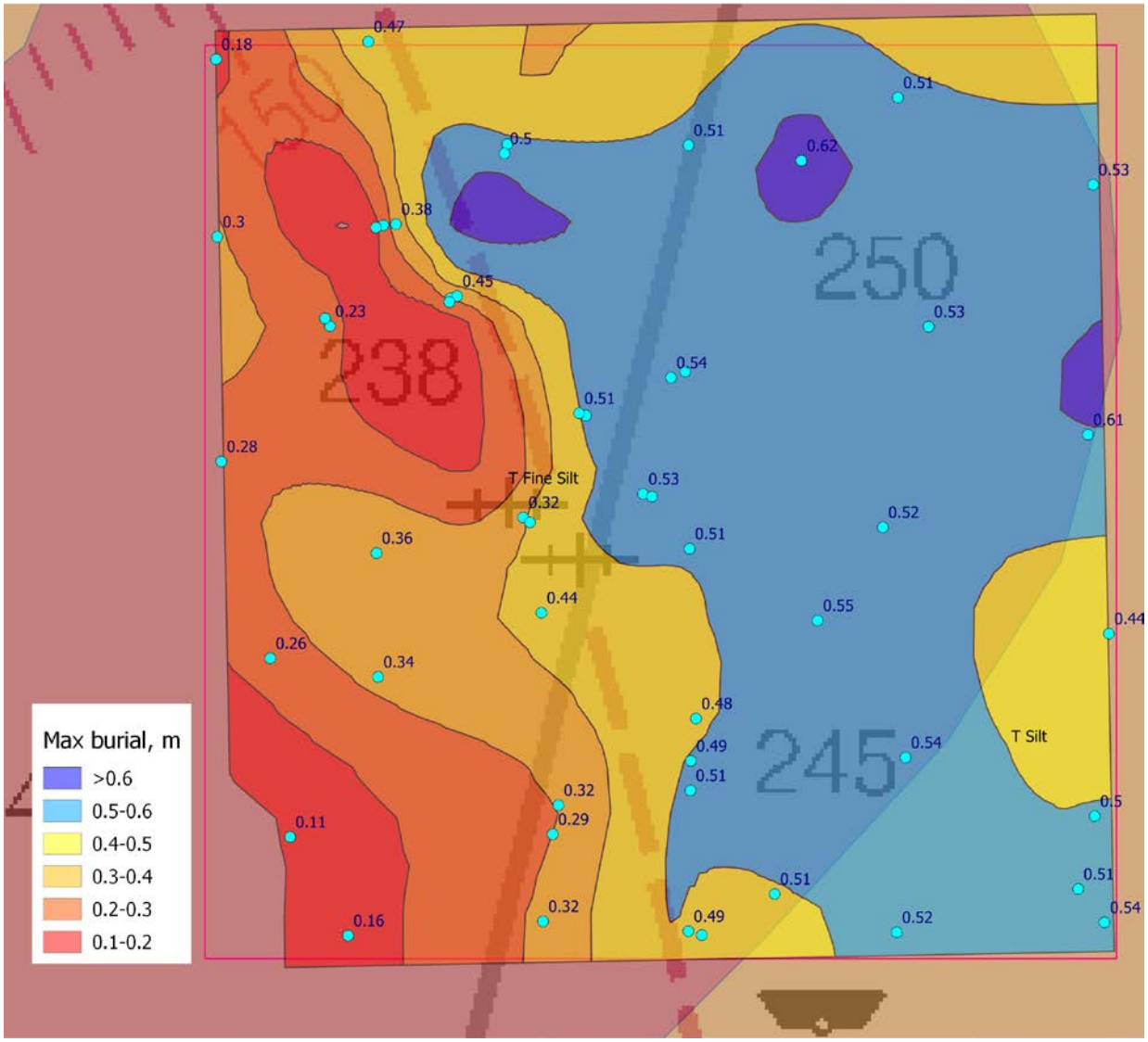


**Fig. 10 Contours of maximum burial depth (STING 70mm), Box 3.1nmi. Individual STING maximum burial values are shown for each station. Shading is assigned by using an average value between two adjacent contour lines. NAVOCEANO sediment data chart is included as an overlay, with majority of Box 3.1nmi defined as Terrigenous Fine Silt. All burial depths are in meters.**

## Summary

In summary, the overall shear strength of the sediment encountered in Box 5 is significantly lower than that in Box 3.1, with no observable presence of sandy layers in much of the box. This results in higher impact burial values and a larger area where these high values may be found. Box 3.1, on the other hand, contains not only sediment that appears coarser (mostly silt, vs. mostly clay), but also includes many locations with significant sandy layering, which severely impedes impact penetration burial.

A preferred area of the softest sediment with greatest potential for high impact burial may thus be identified in Box 5, as shown approximately in Fig. 8, occupying the majority of the initial box and somewhat away from the sandy mound, found near the Northern boundary. The coordinates of this preferred box are as follows:

| Field | Lat, deg | Lon, deg |
|---|---|---|
| NW | 42.38782 | -70.57281 |
| NE | 42.39073 | -70.55382 |
| SE | 42.37955 | -70.55006 |
| SW | 42.37628 | -70.56912 |

A slow transition into more silty sediments begins West and South-West of this identified area, where STING-70 penetration burial depths, and therefore expected burials of larger objects, begin to decline gradually.

## Acknowledgments

Assistance in STING deployments by the personnel of NRL Code 7130, the crew of r/v Matthew Hughes (Boston Harbor Cruises), and the staff of Bluefin Robotics Co. is acknowledged.

## References


Abelev, A. (2014), *Sediment strength characteristics and impact burial conditions in approach to Boston Harbor*, Memorandum report, Naval Research Laboratory, Washington,.

Alperin, M. J., I. B. Suayah, L. K. Benninger, and C. S. Martens (2002), Modern organic carbon burial fluxes, recent sedimentation rates, and particle mixing rates from the upper continental slope near Cape Hatteras, North Carolina (USA), *Deep Sea Res. Part II Top. Stud. Oceanogr.*, *49*(20), 4645–4665, doi:10.1016/S0967-0645(02)00133-9.

Crusius, J., M. H. Bothner, and C. K. Sommerfield (2004), Bioturbation depths, rates and processes in Massachusetts Bay sediments inferred from modeling of 210Pb and 239 + 240Pu profiles, *Estuar. Coast. Shelf Sci.*, *61*(4), 643–655, doi:10.1016/j.ecss.2004.07.005.

Jasco Research Ltd. (2002), *STING Mk.II - Underwater Sediment Bearing Strength Probe. User's Manual*, R-Hut, University of Victoria Campus Victoria, British Columbia.

Mulhearn, P. J. (2002), *Influences of penetrometer probe tip geometry on bearing strength estimates for mine burial prediction*, DTIC Document. online Available from: http://oai.dtic.mil/oai/oai?verb=getRecord&metadataPrefix=html&identifier=ADA402610 (Accessed 13 December 2013)

Stoll, D., Y.-F. Sun, and I. Bitte (2007), Seafloor properties from penetrometer tests, *Ocean. Eng. IEEE J. Of*, *32*(1), 57–63.

## Appendix A STING data – bearing strength profiles with depth. Bo3.1nmi

Note: negative bearing strength values that appear near zero sediment depth in some drops (or averages) are artifacts of STING software processing or minor inconsistencies in sensor calibrations and have no physical meaning. This is possible in cases of very soft surficial material (as it is here), when the water-sediment interface is often not well defined and is difficult to determine from deceleration records (either via native automated STING processing or by manual selection). Practically, these negative values should, of course, be all positive. In all cases, these inconsistencies are minor and are well within the overall accuracy of the instrument in sediments of this type.

Station 2:

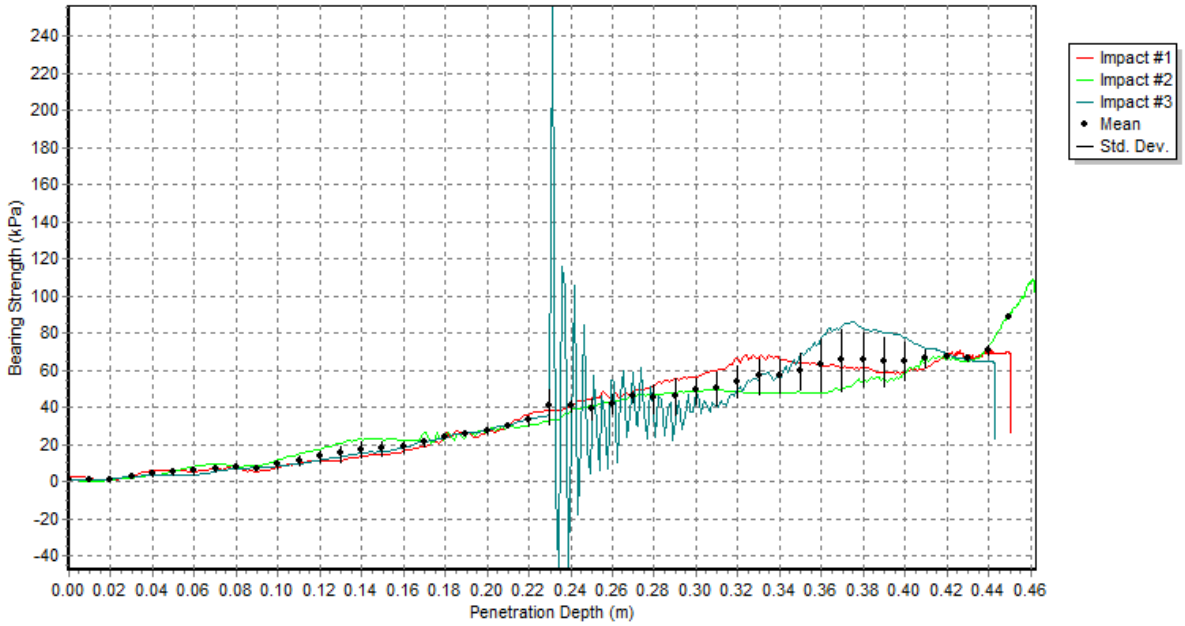


Station 3:

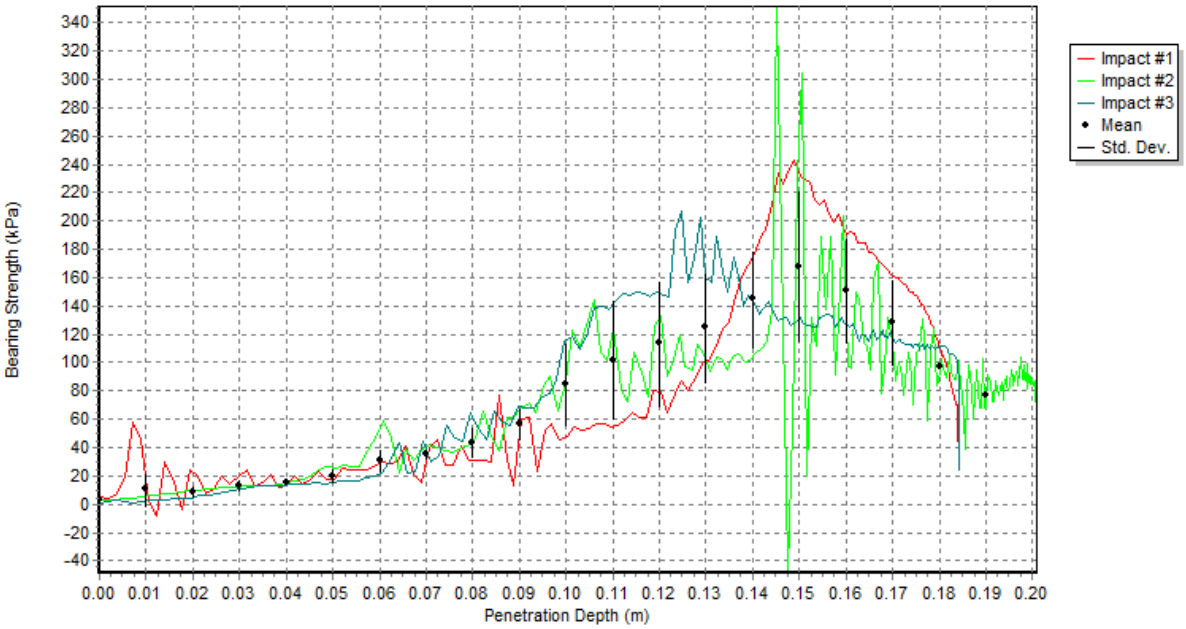

Station: 5

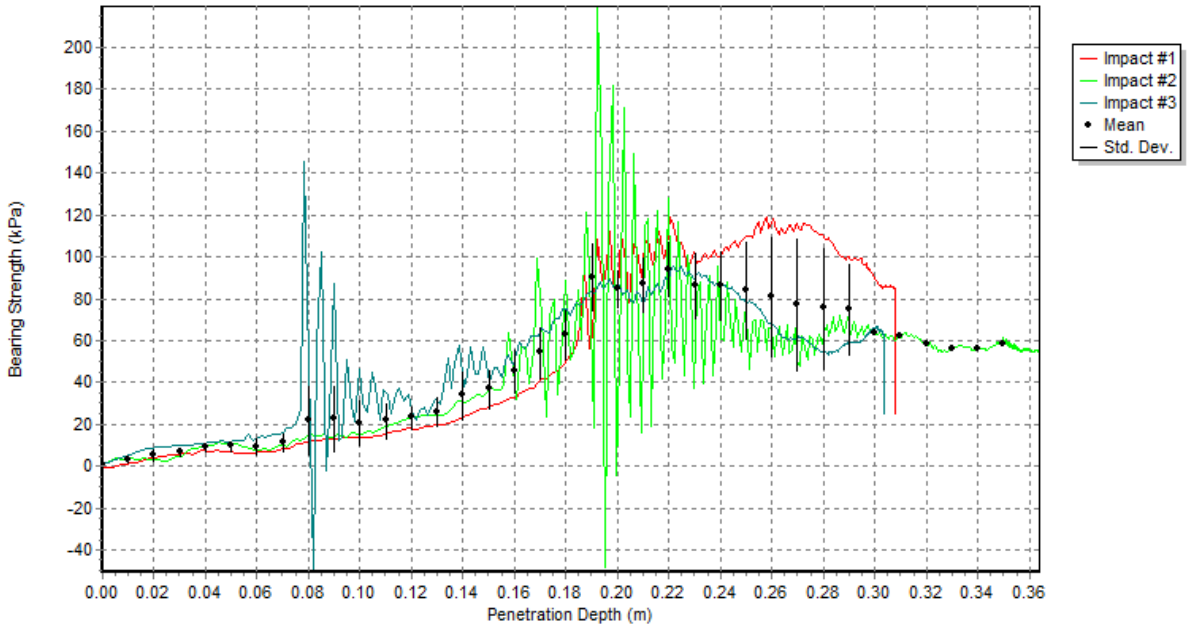


Station: 6

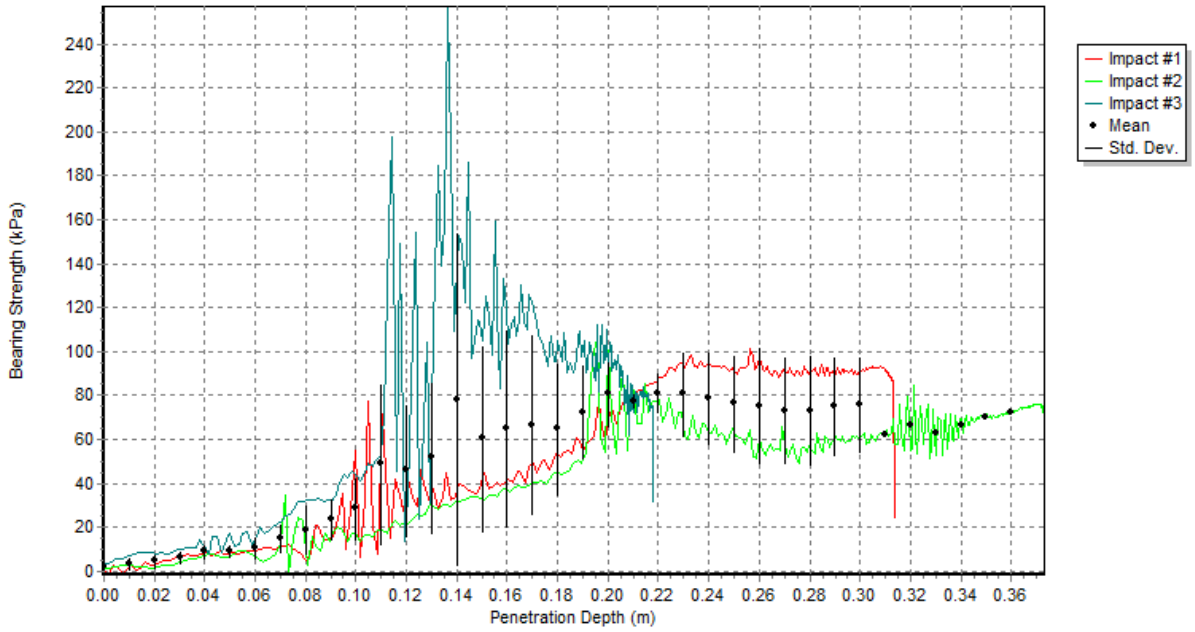

Station: 8

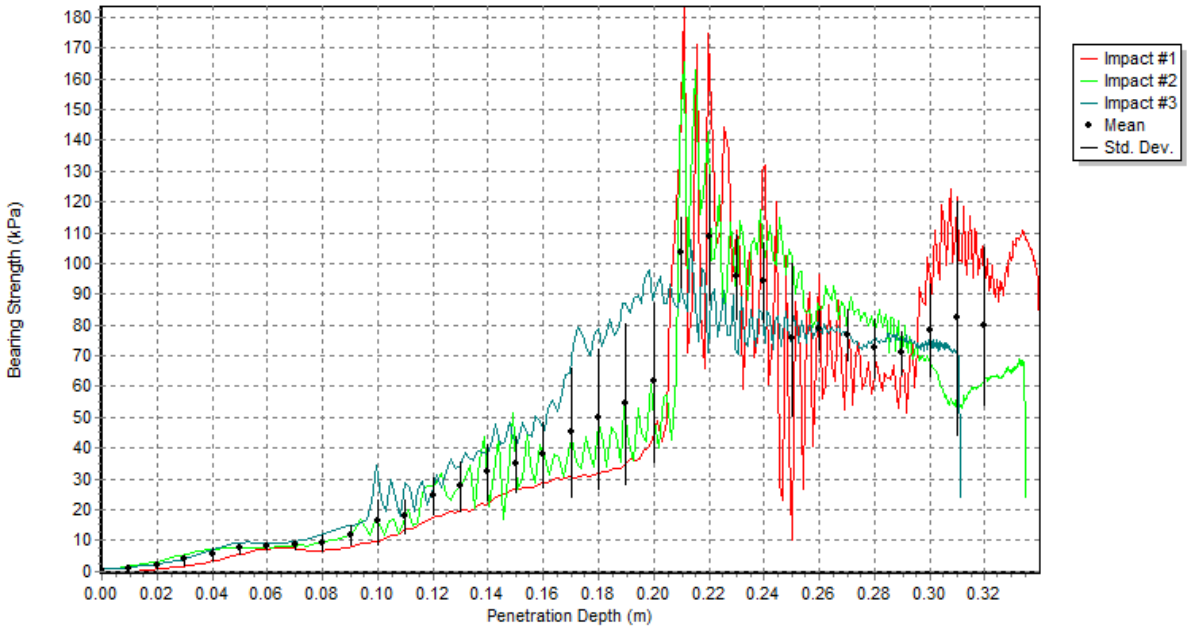


Station: 9

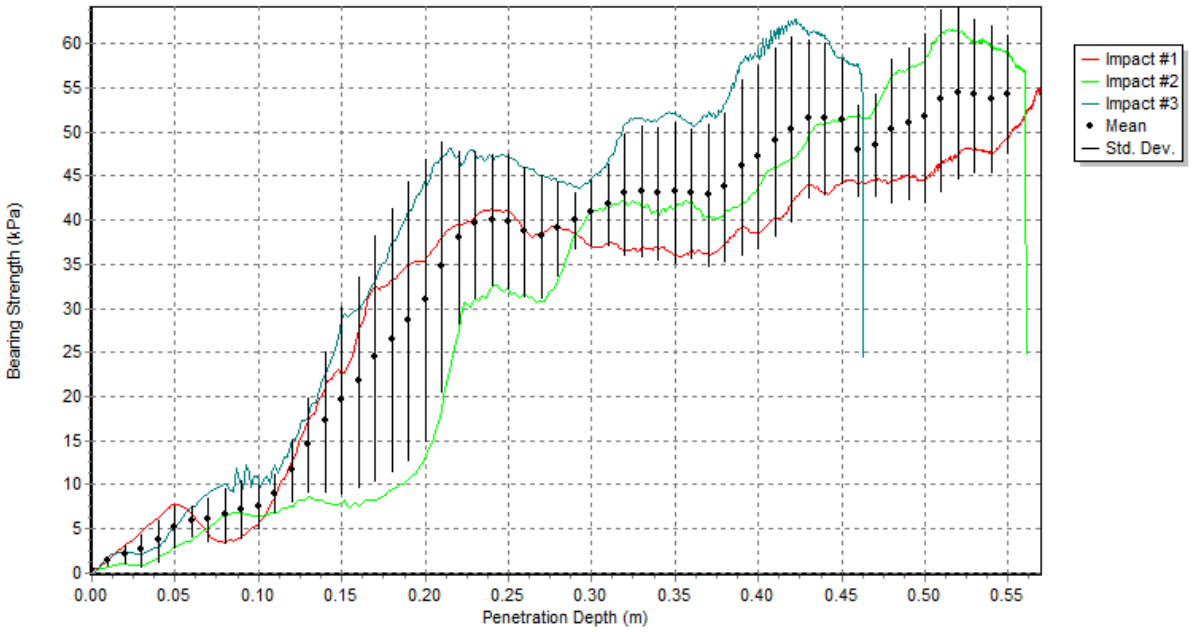

Station 10:

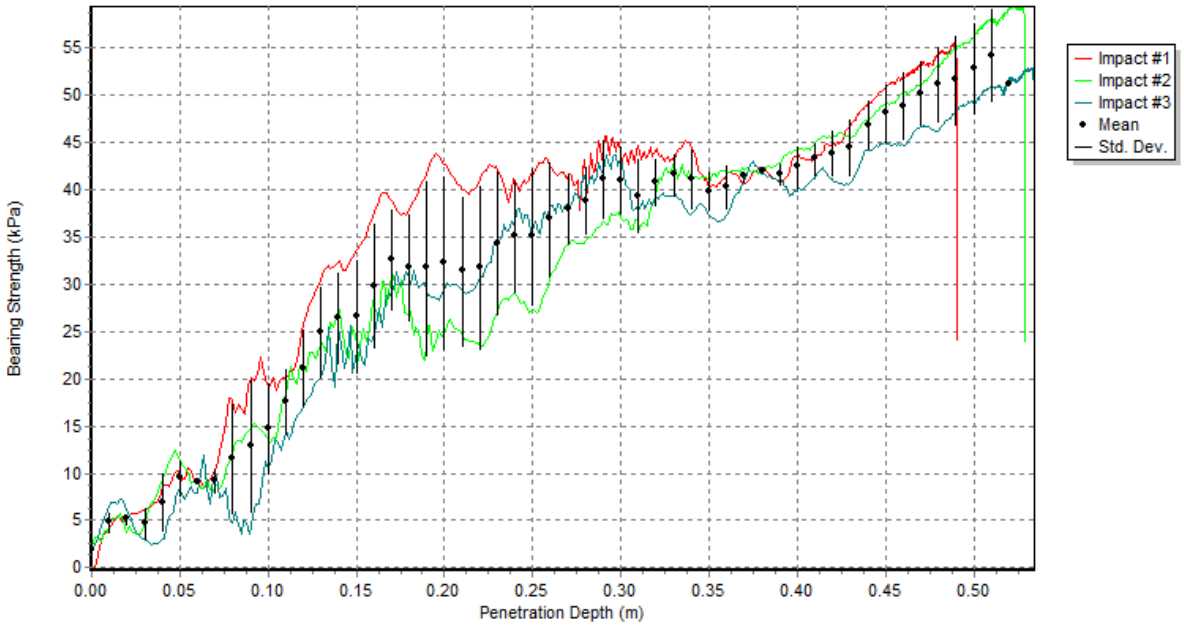


Station 12:

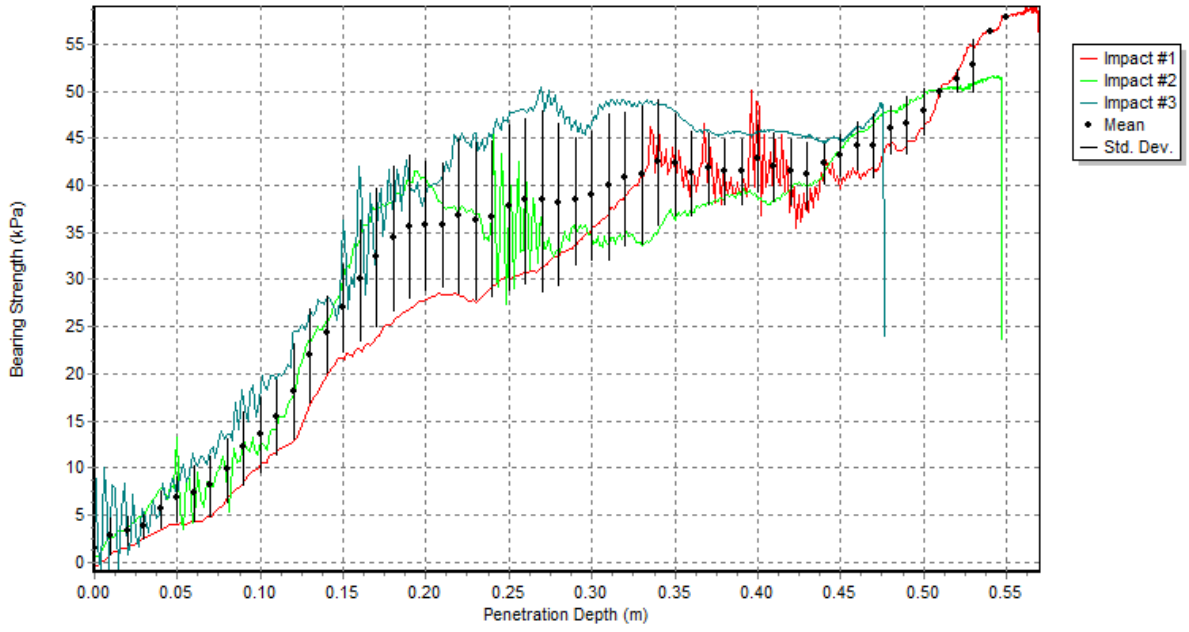

Station 14:

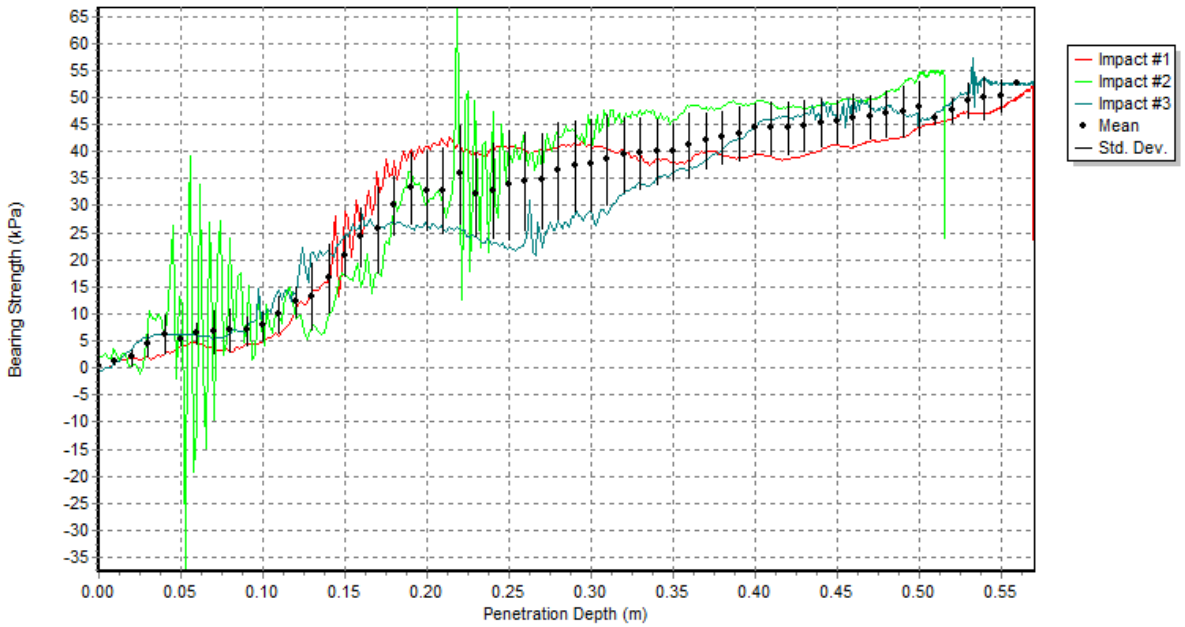


Station 15:

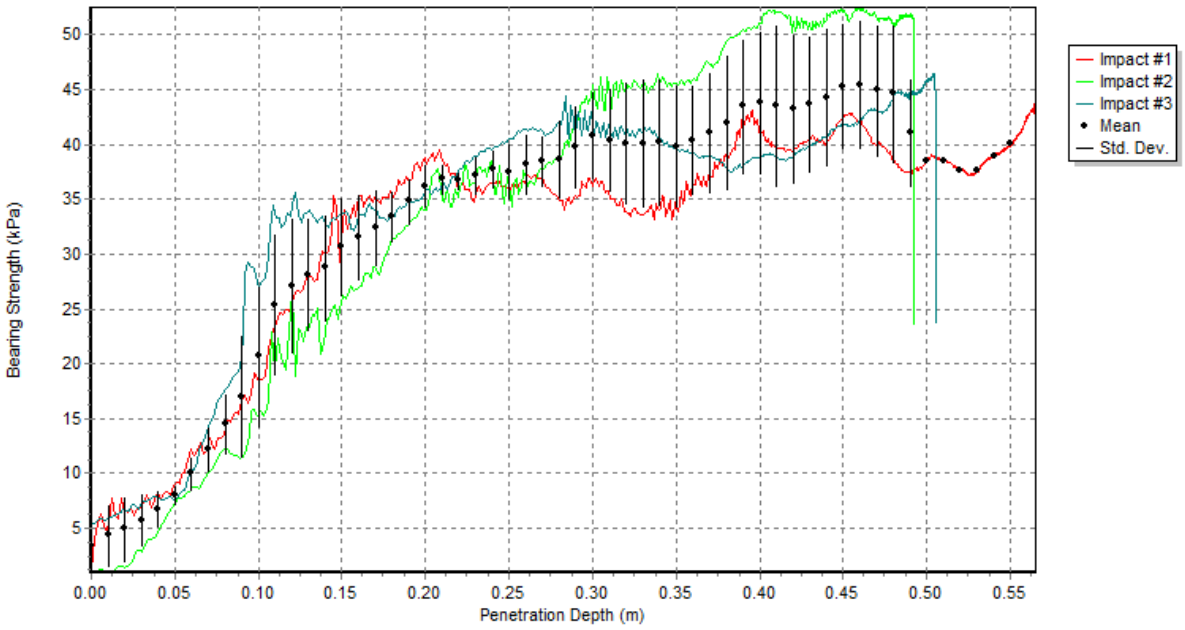

Station 16:

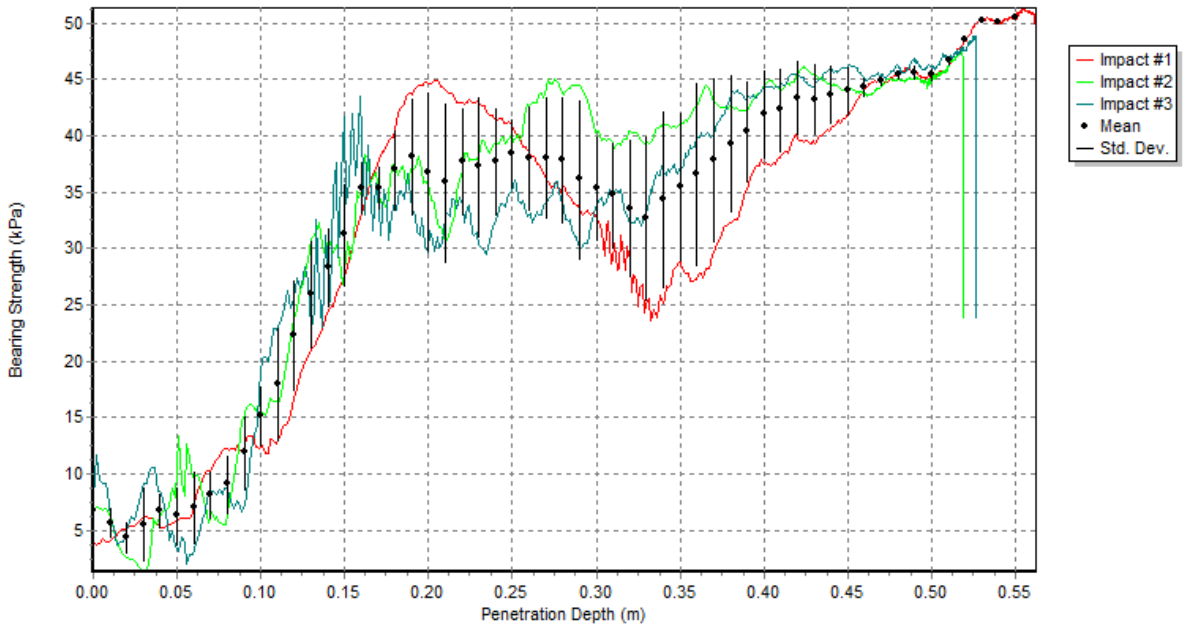


Station 17:

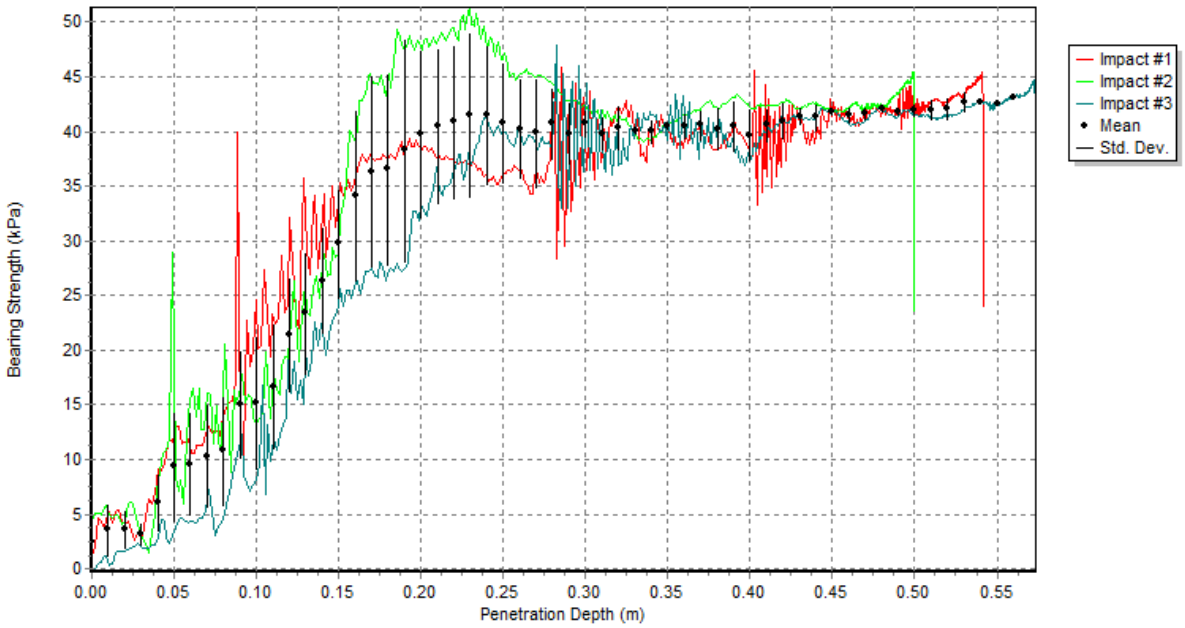

Station 18:

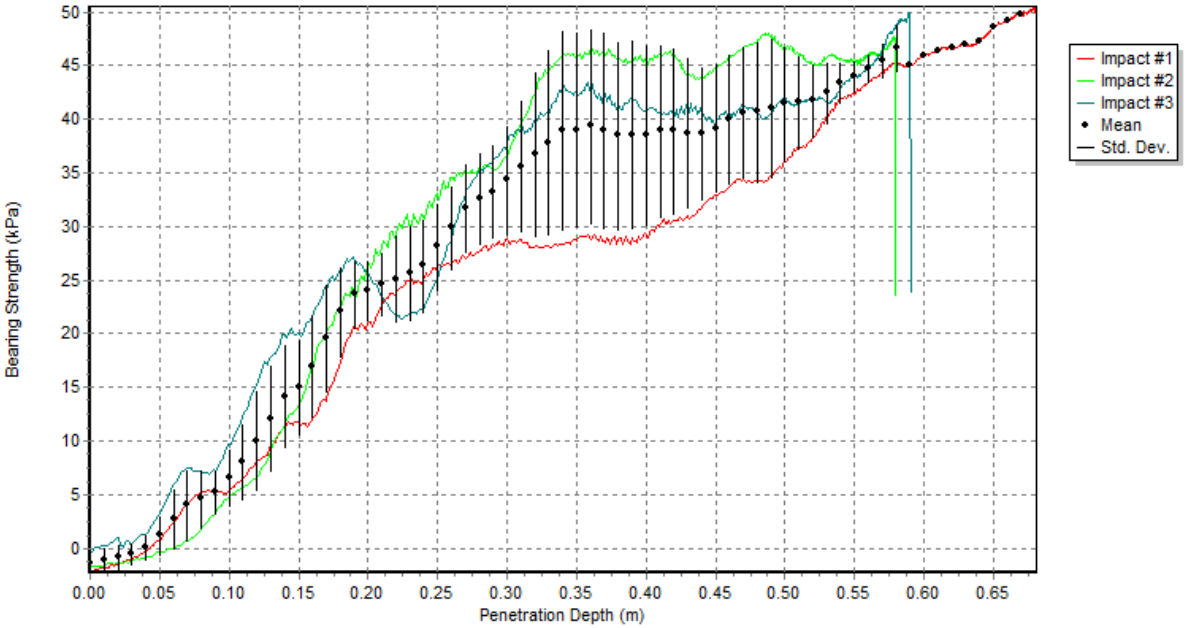


Station 19:

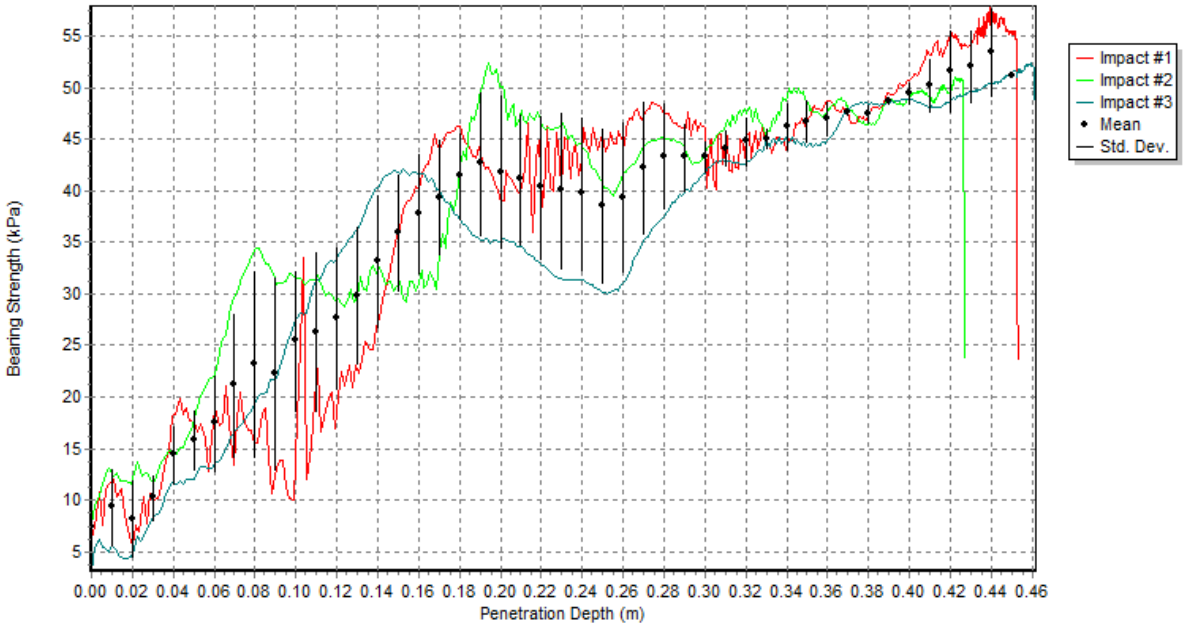

Station 21:

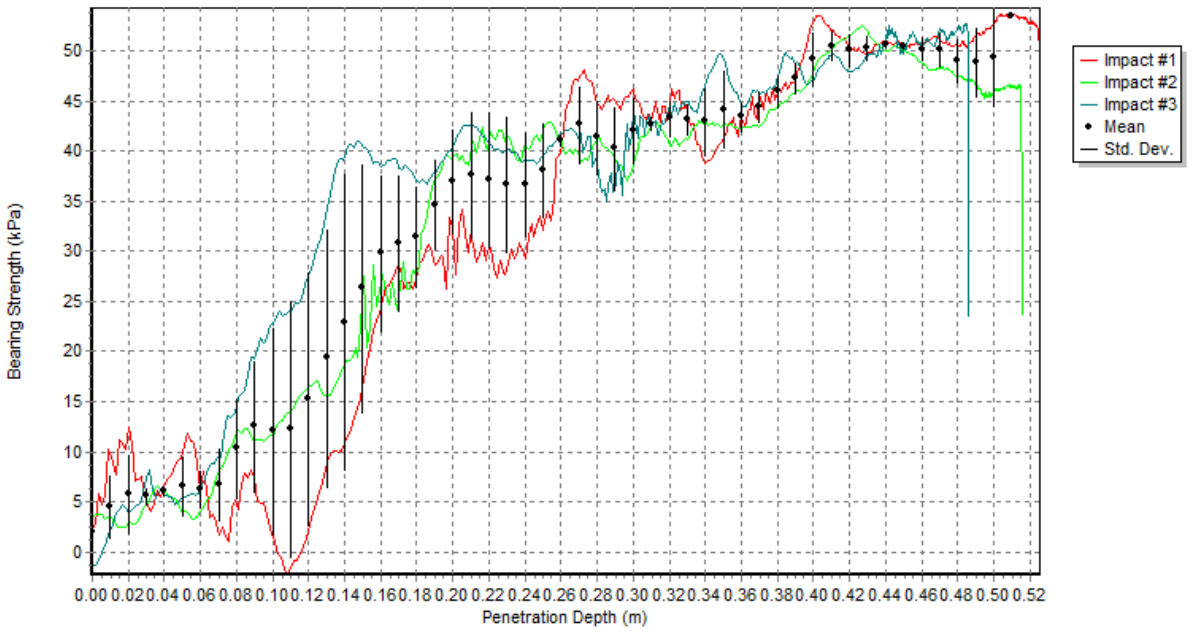


Station 22:

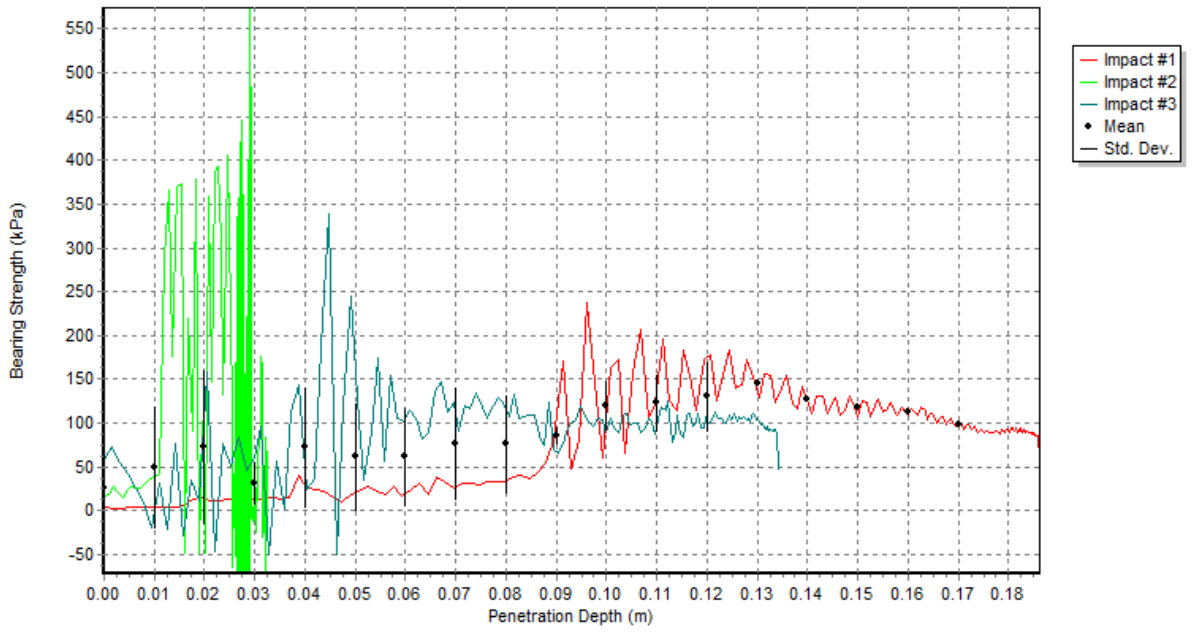

Station 23:

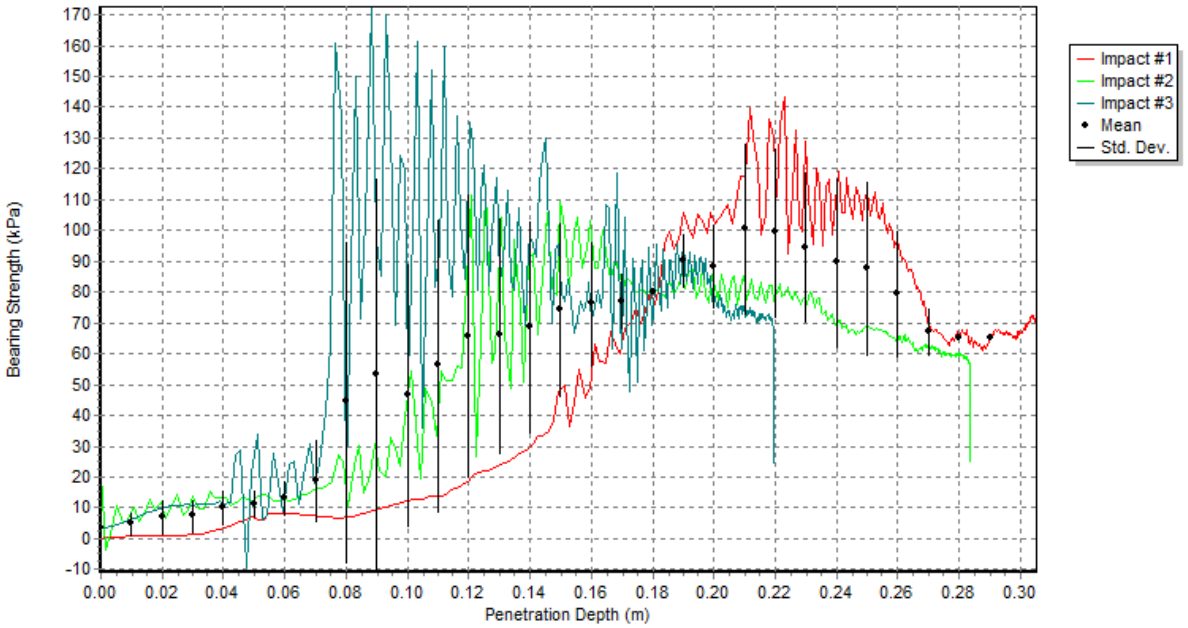


Station 24:

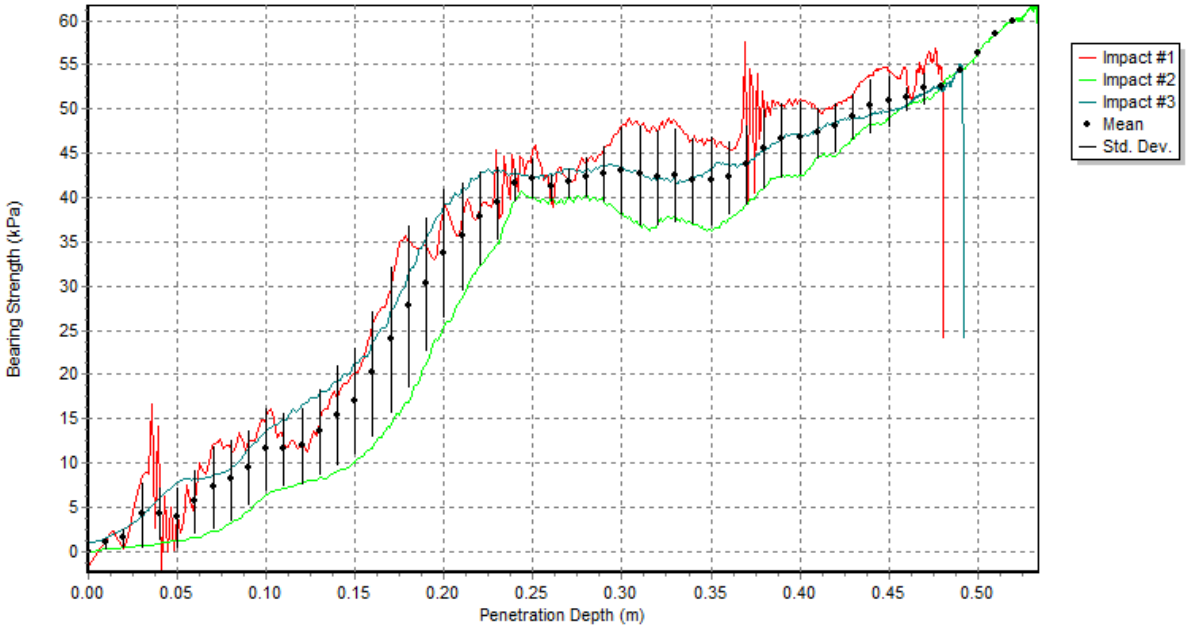

Station 25:

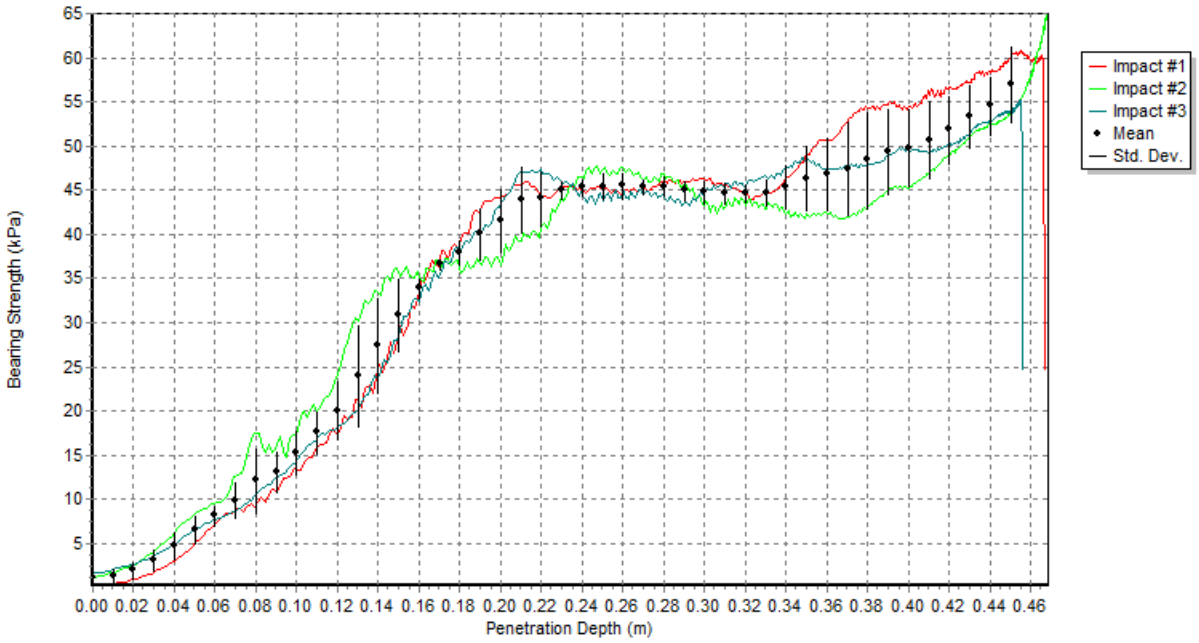


Station 26:

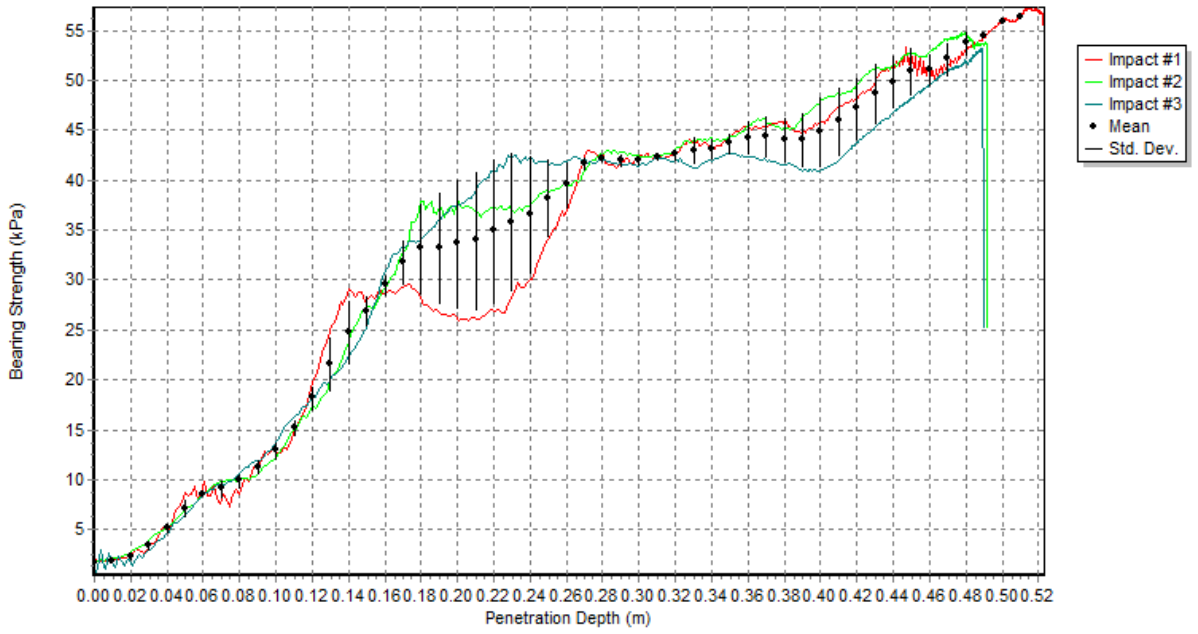

Station 27:

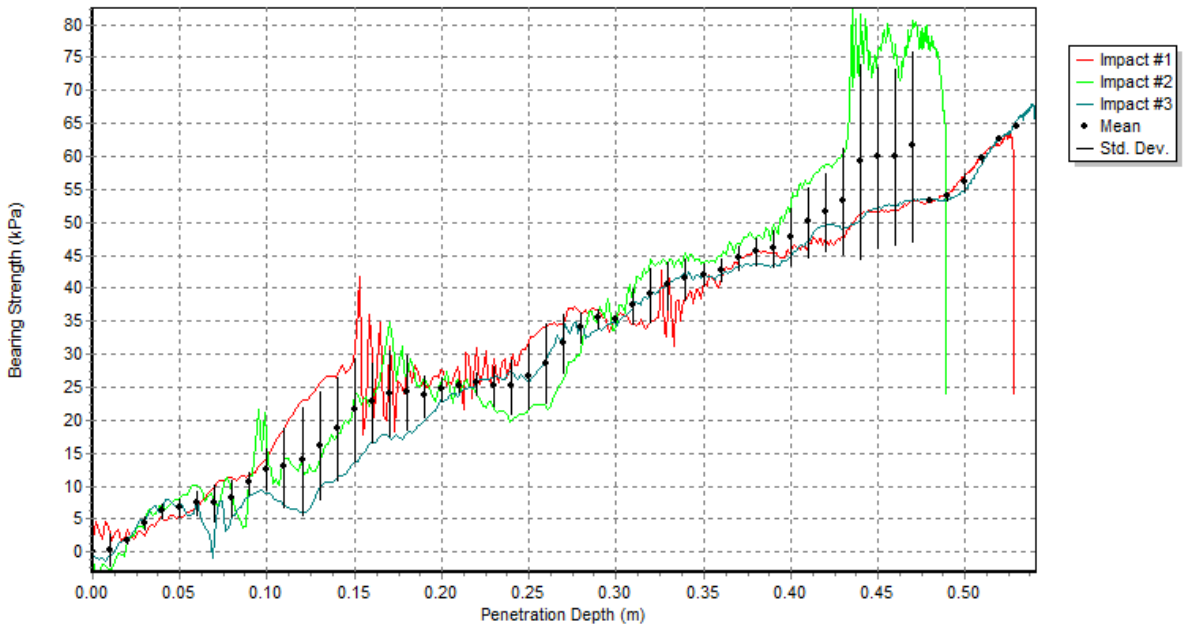


Station 29:

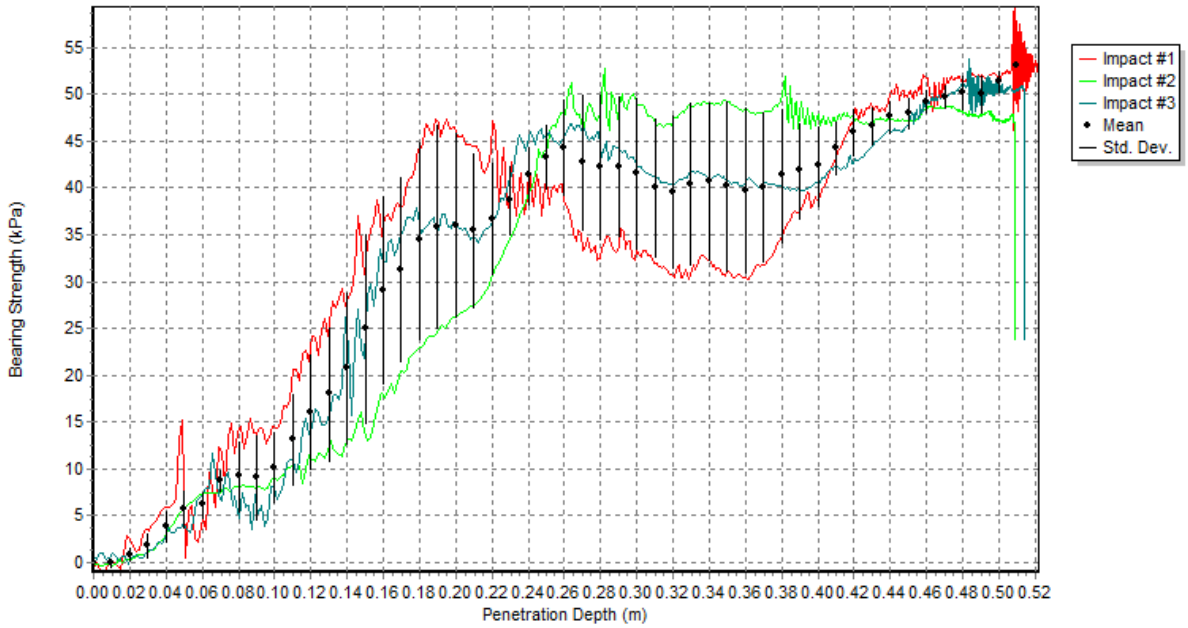

Station 30:

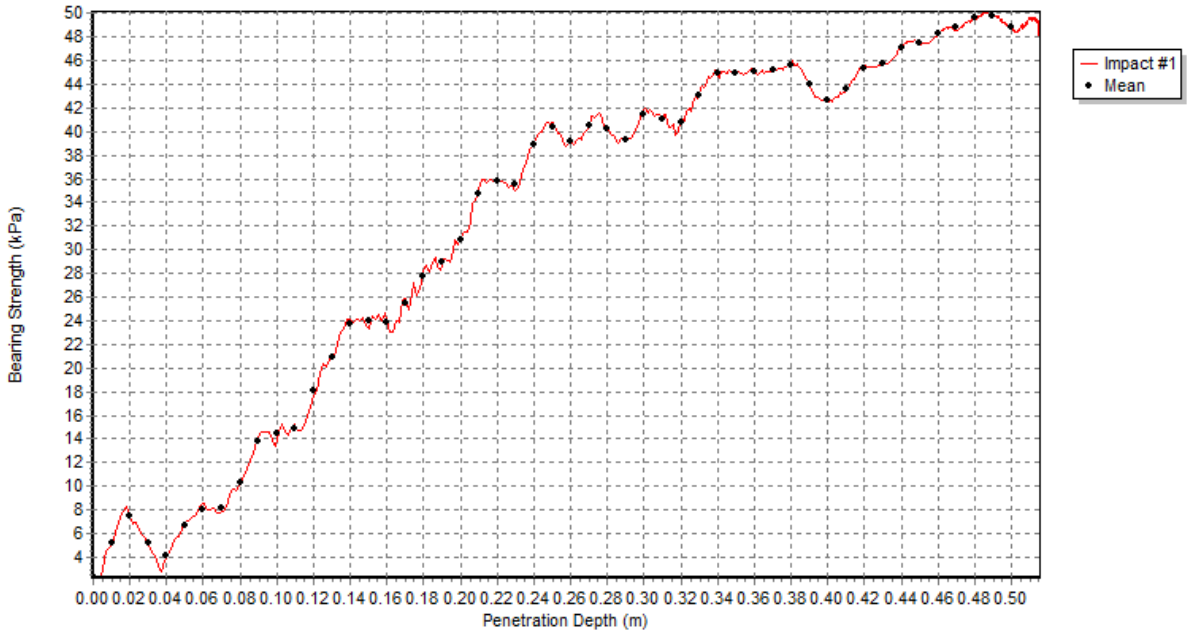


Station 31:

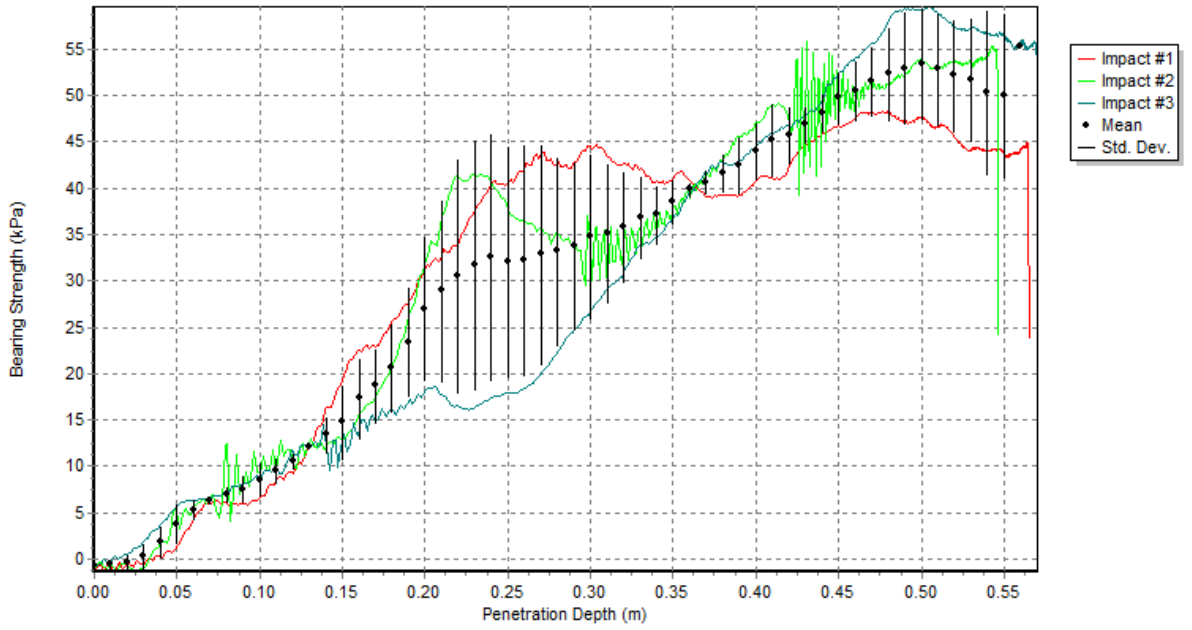

Station 32:

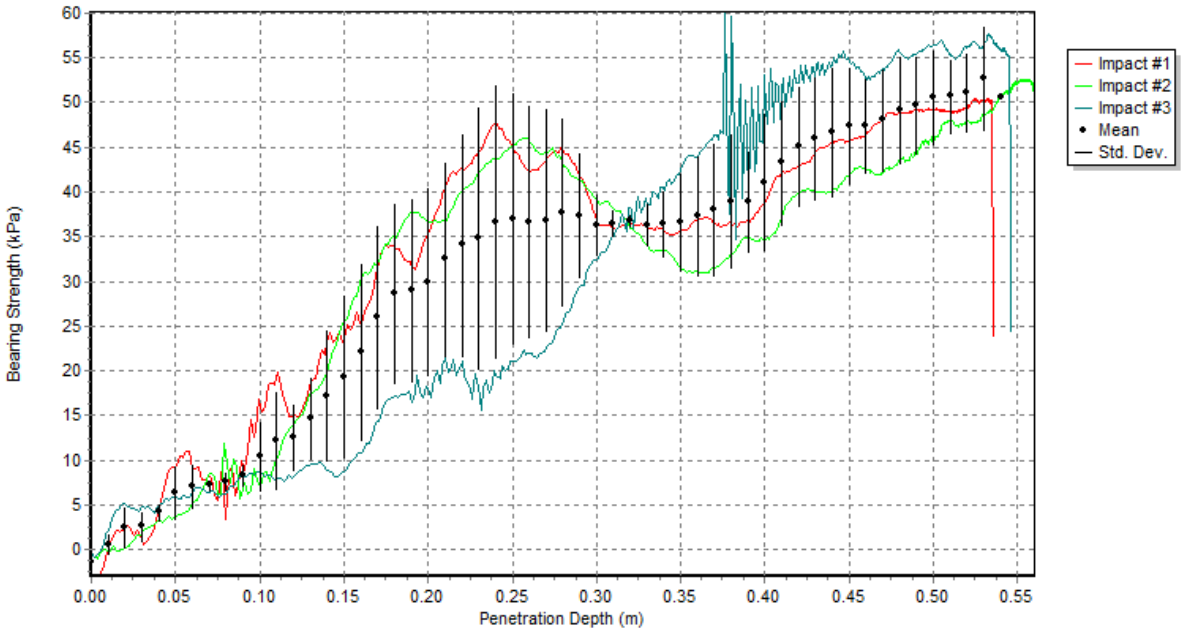


Station 33:

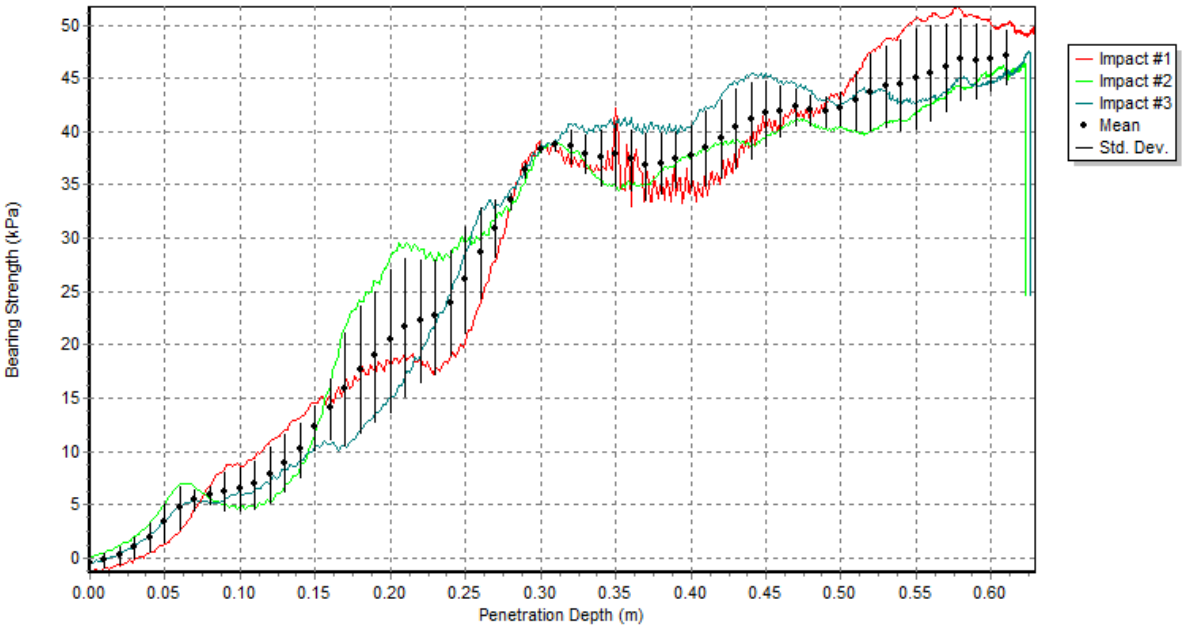

Station 34:

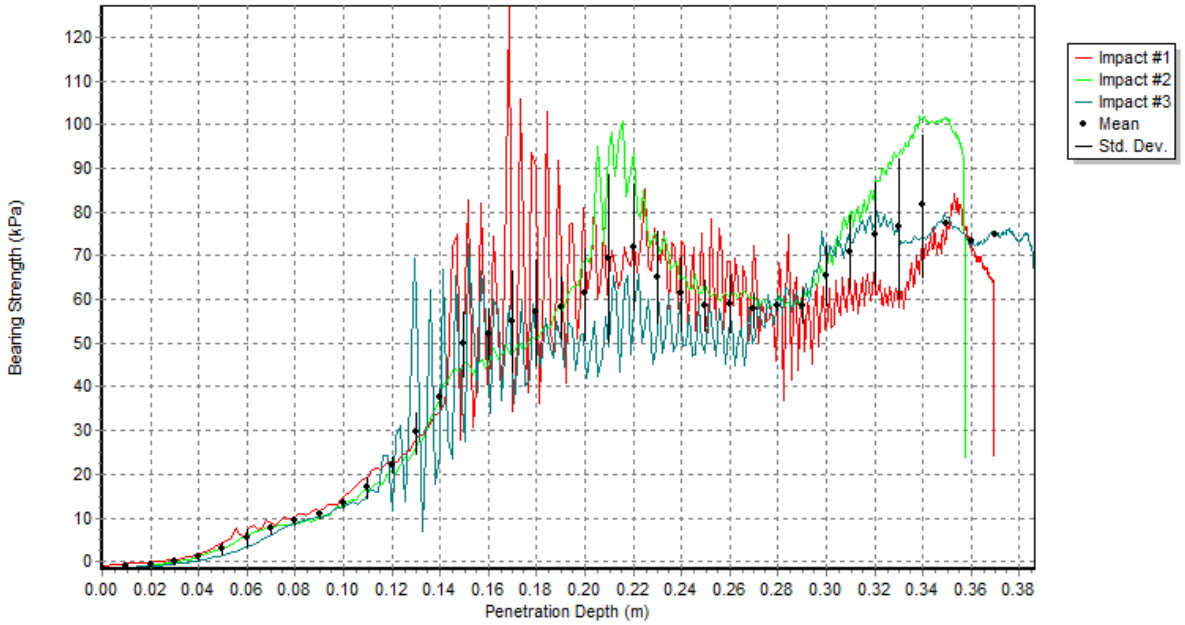


Station 35:

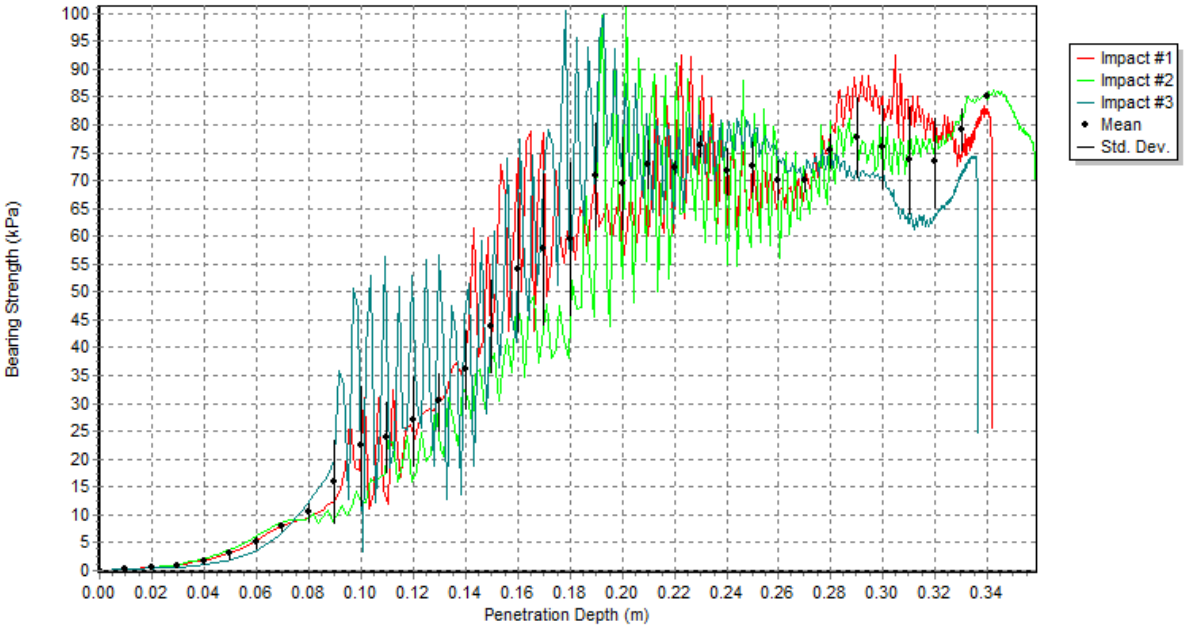

Station 36:

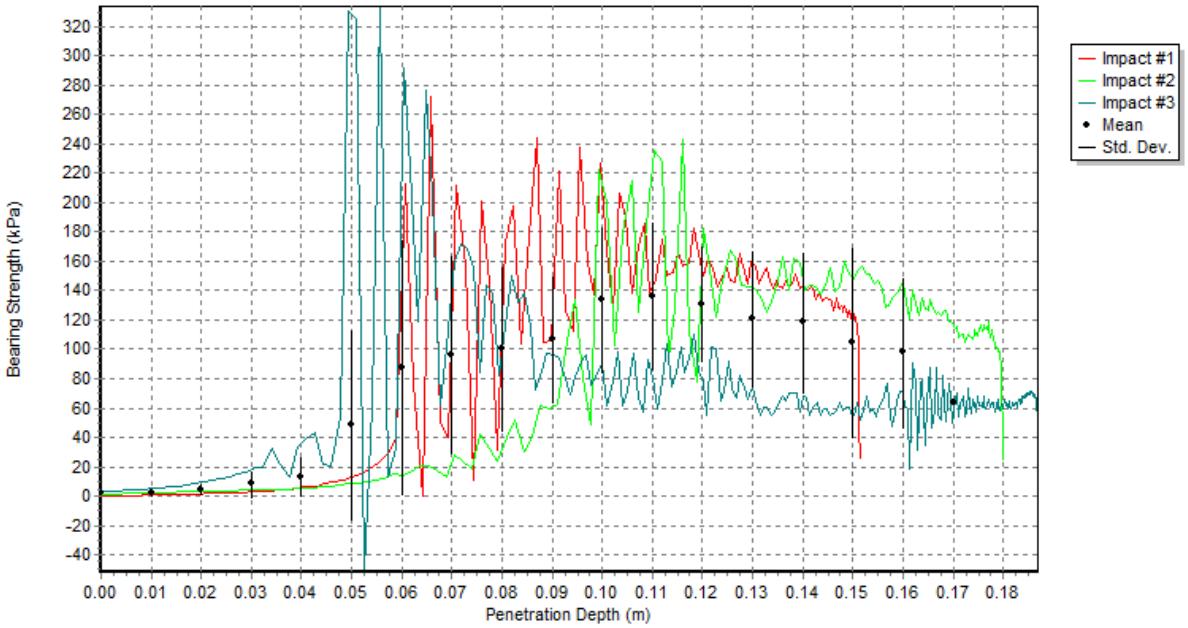


Station 37:

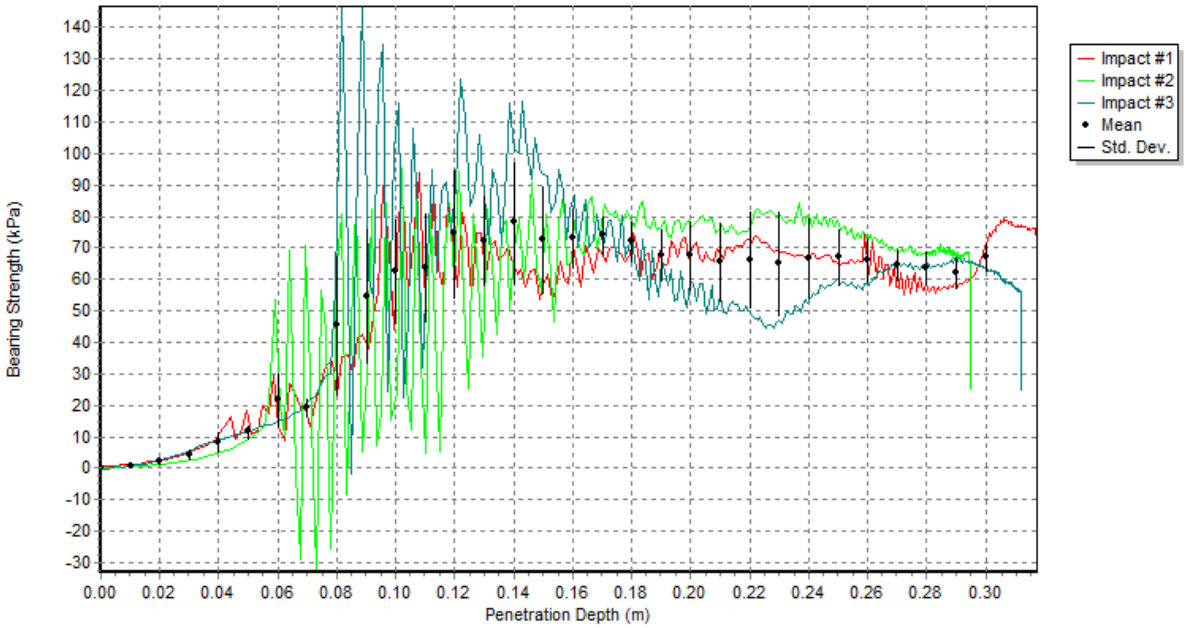

Station 38:

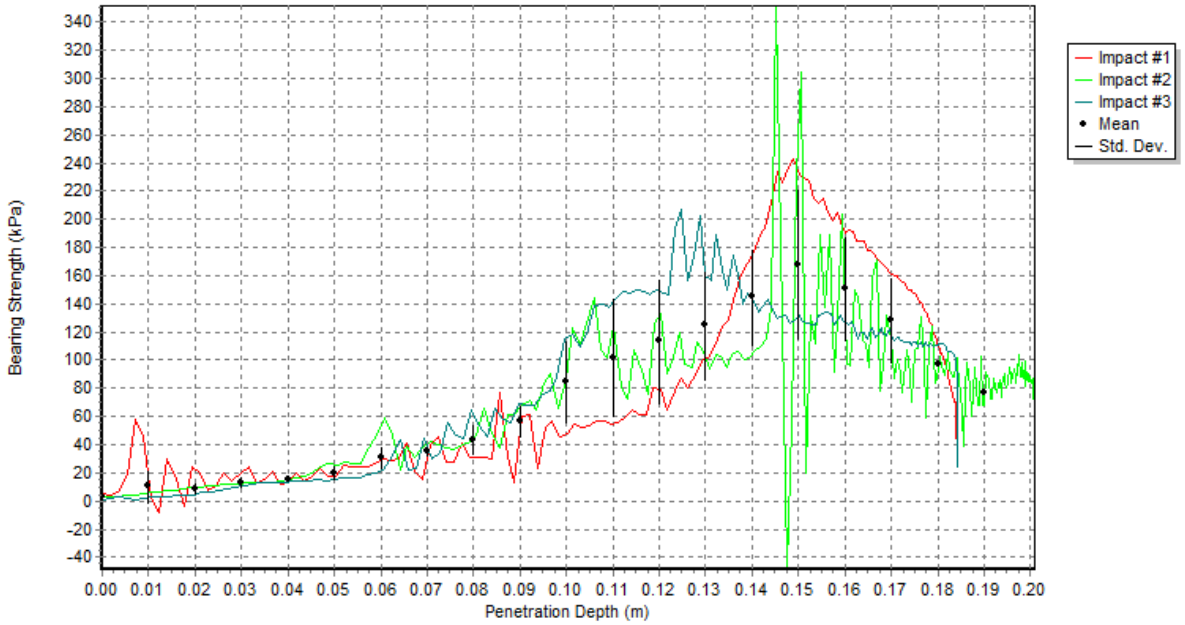


Station 39

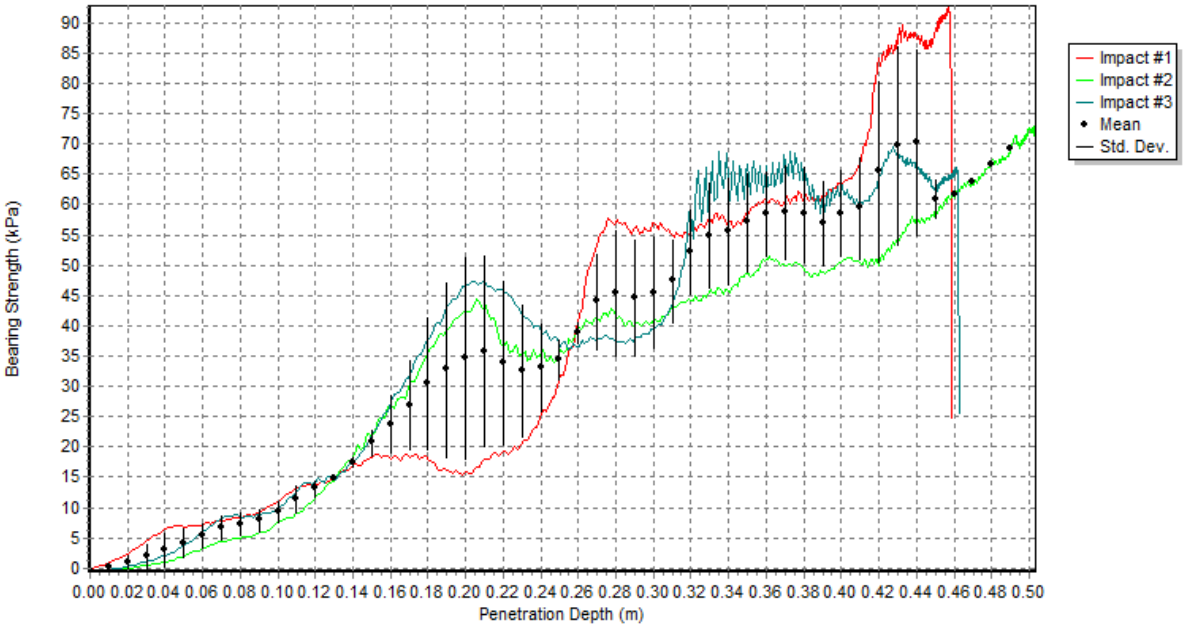

## Appendix B STING data – bearing strength profiles with depth. Box 5.

Note: negative bearing strength values that appear near zero sediment depth in some drops (or averages) are artifacts of STING software processing or minor inconsistencies in sensor calibrations and have no physical meaning. This is possible in cases of very soft surficial material (as it is here), when the water-sediment interface is often not well defined and is difficult to determine from deceleration records (either via native automated STING processing or by manual selection). Practically, these negative values should, of course, be all positive. In all cases, these inconsistencies are minor and are well within the overall accuracy of the instrument in sediments of this type.

Station: 1:

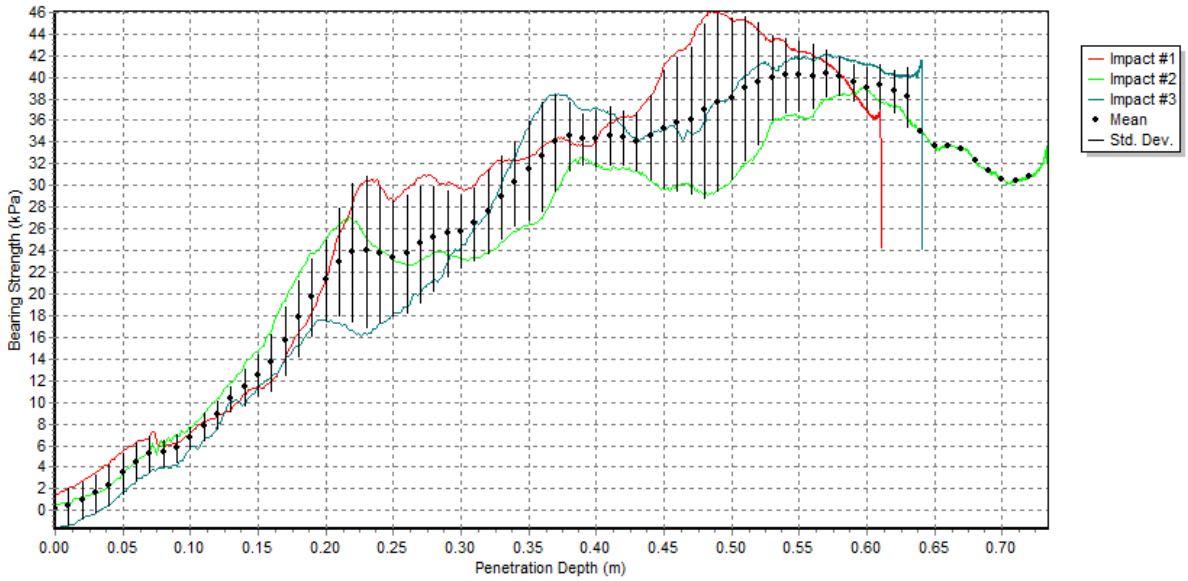


Station 2:

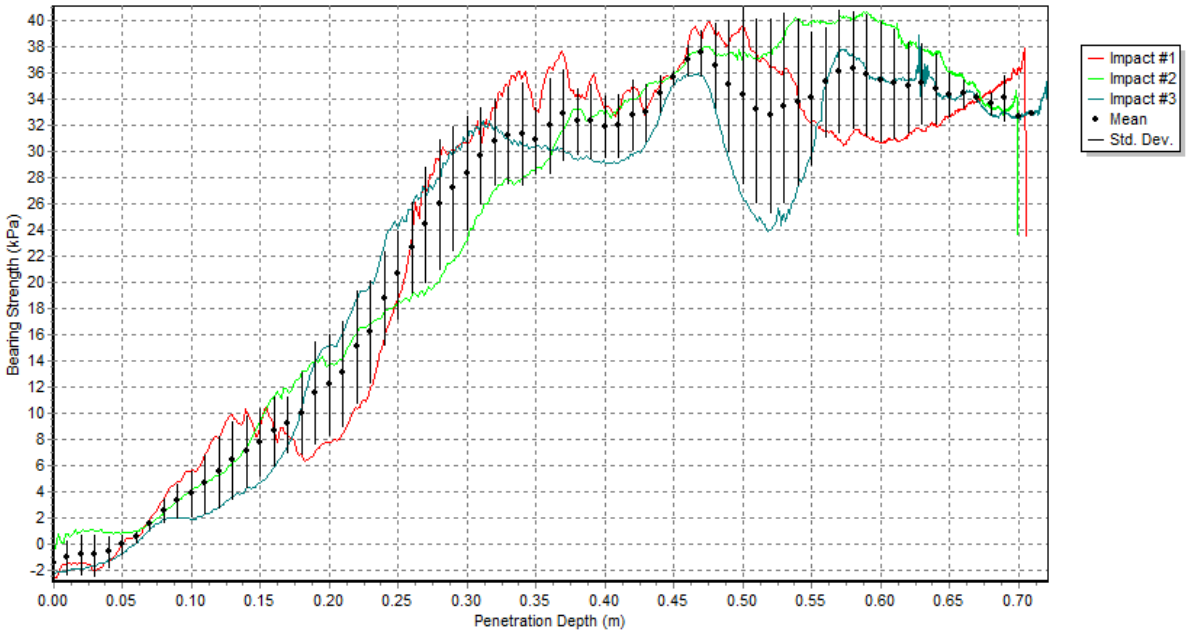

Station 3:

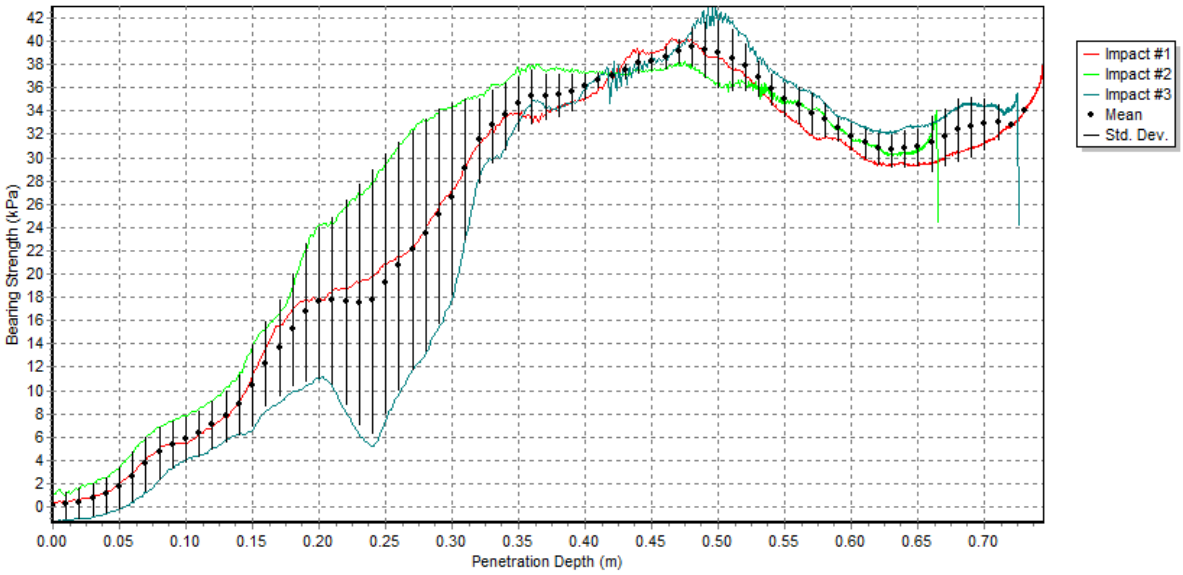


Station 4:

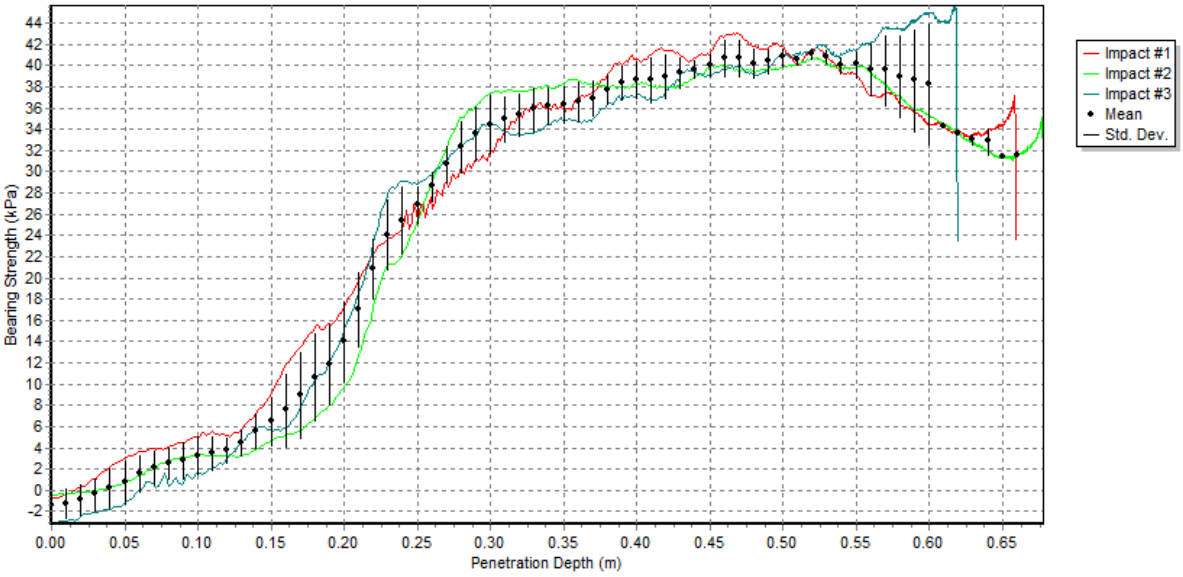

Station 5:

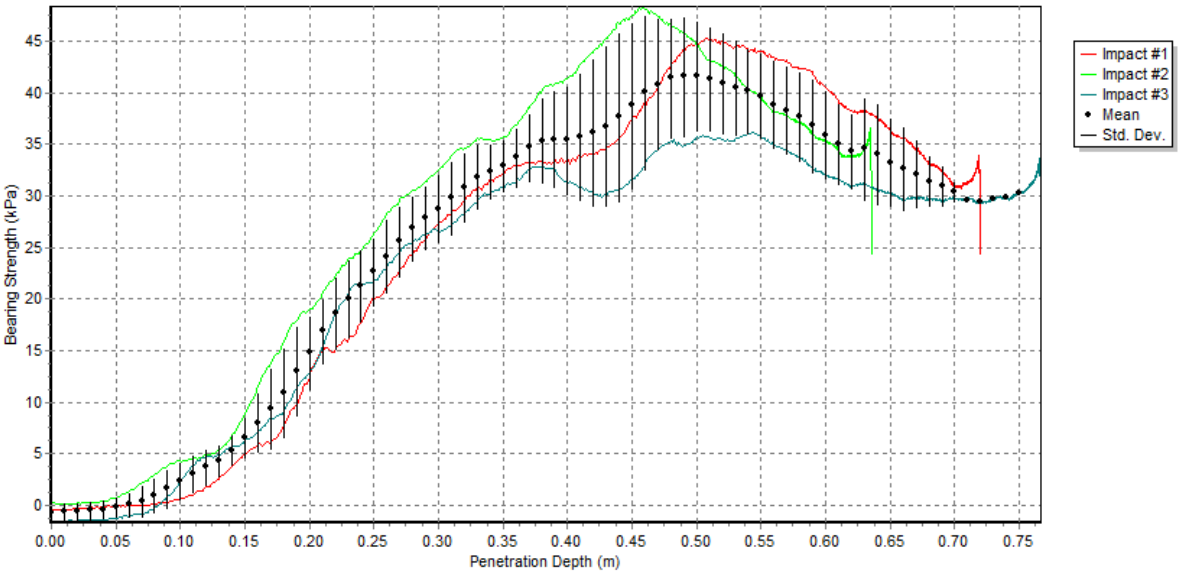


Station 7:

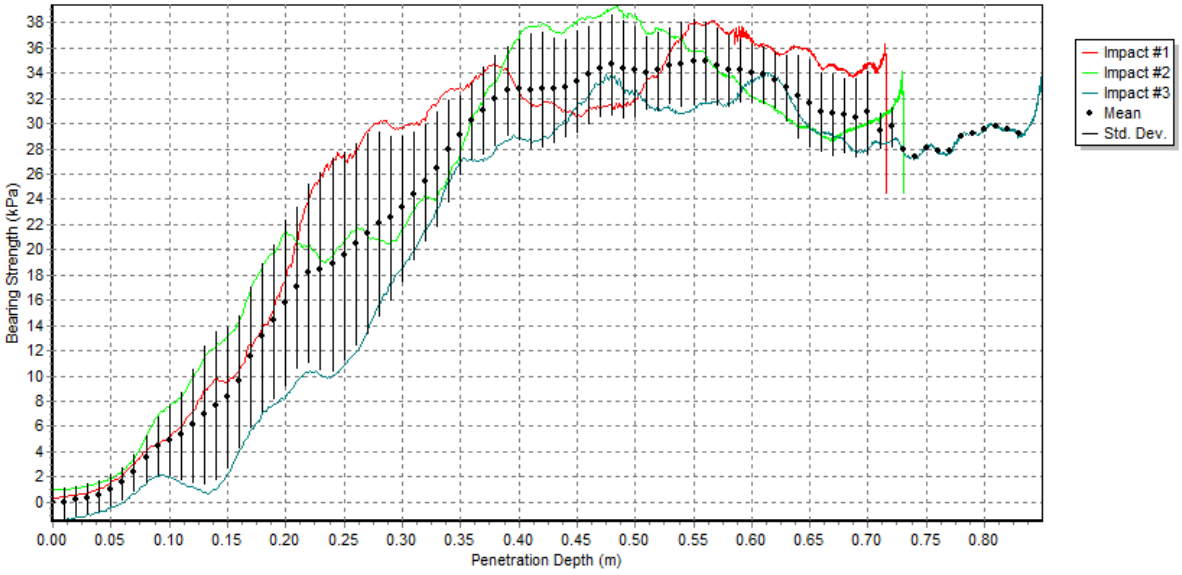

Station 8:

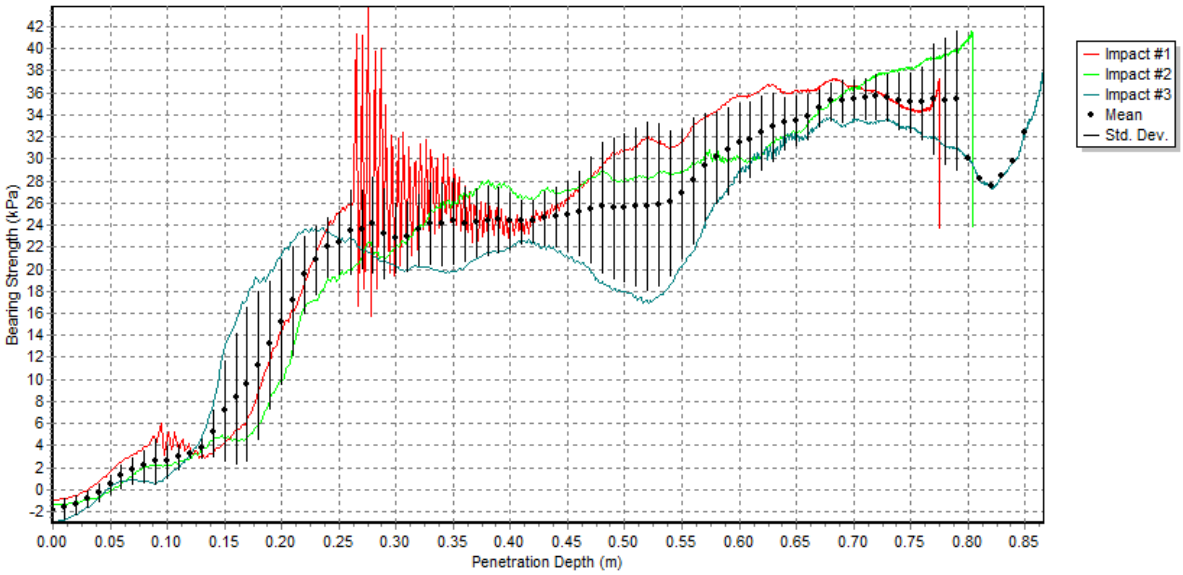


Station 9:

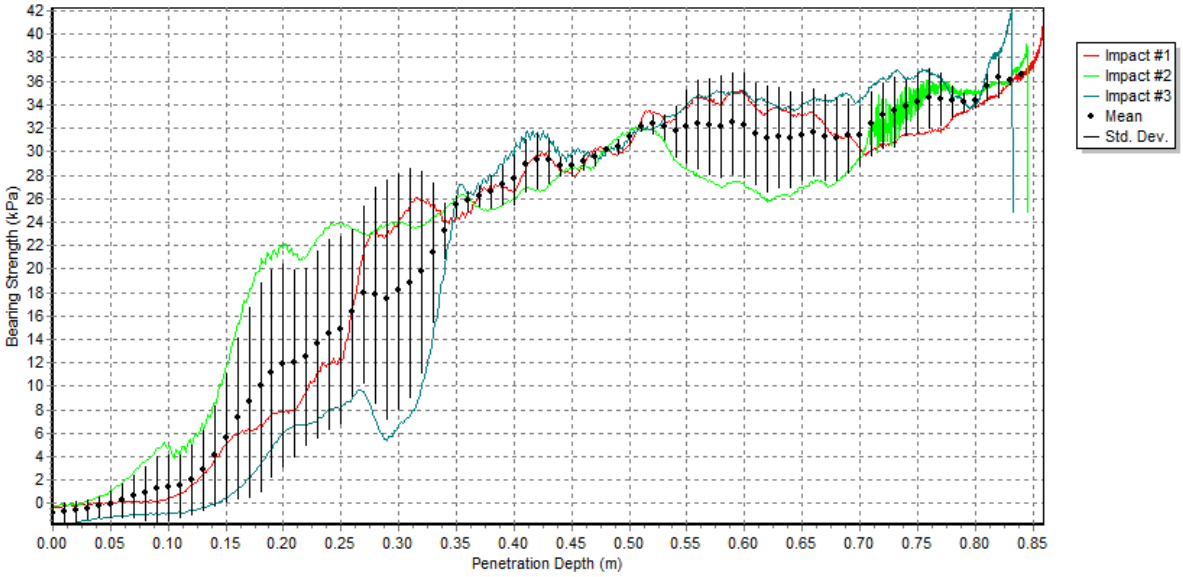

Station 10:

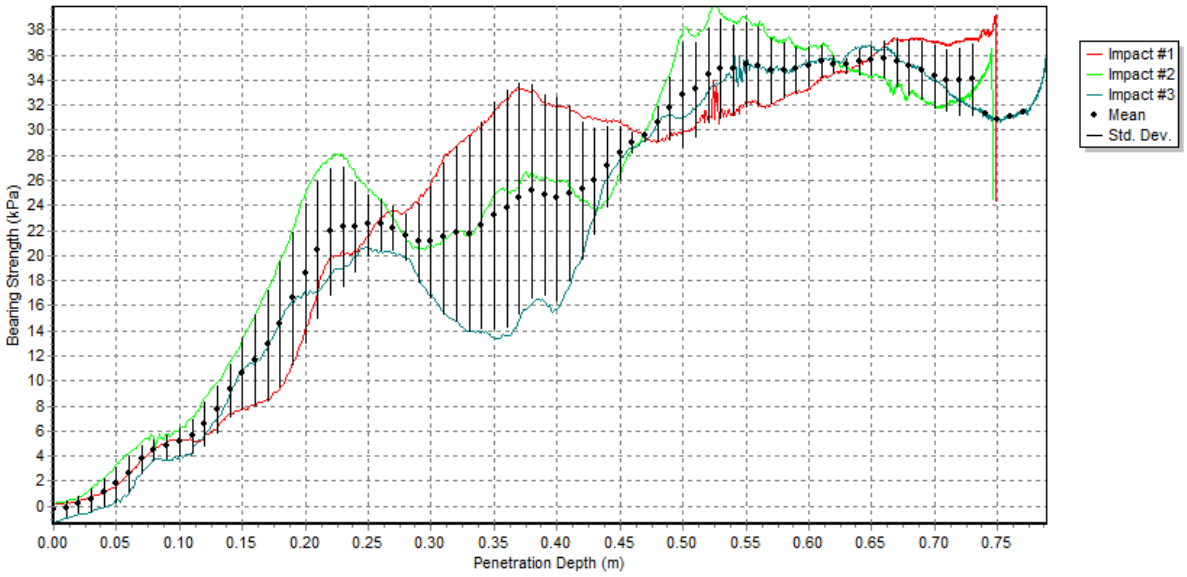


Station 11:

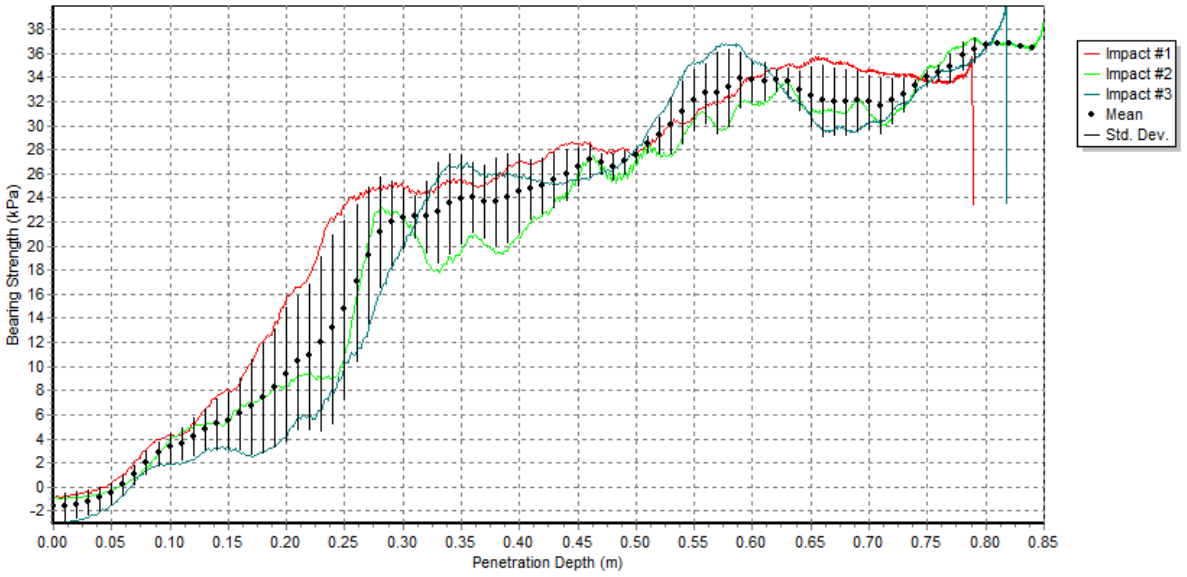

Station 12:

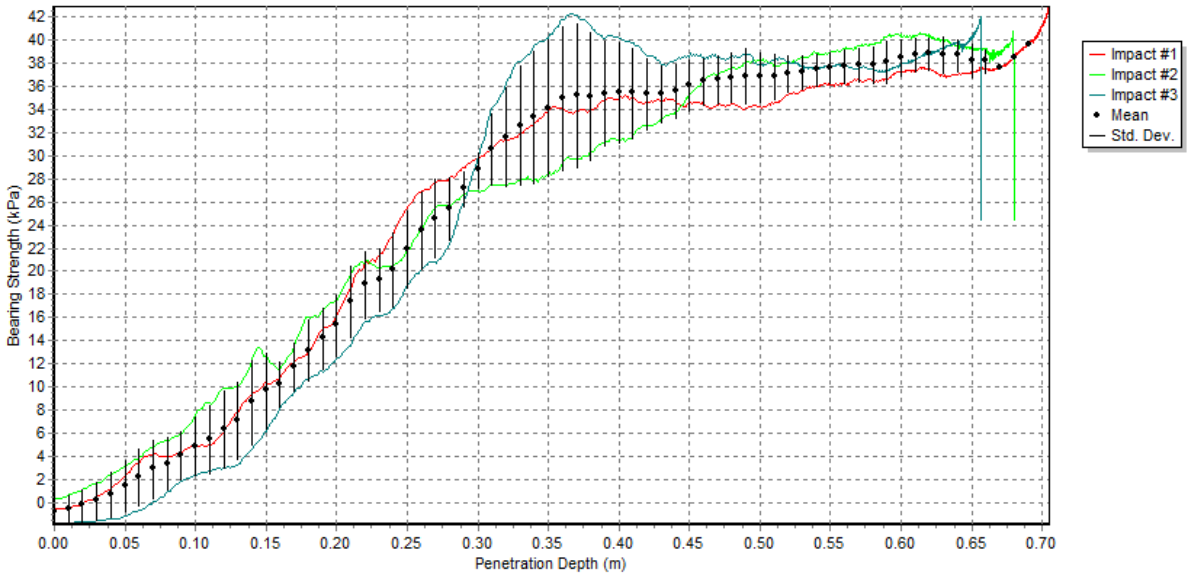


Station 13:

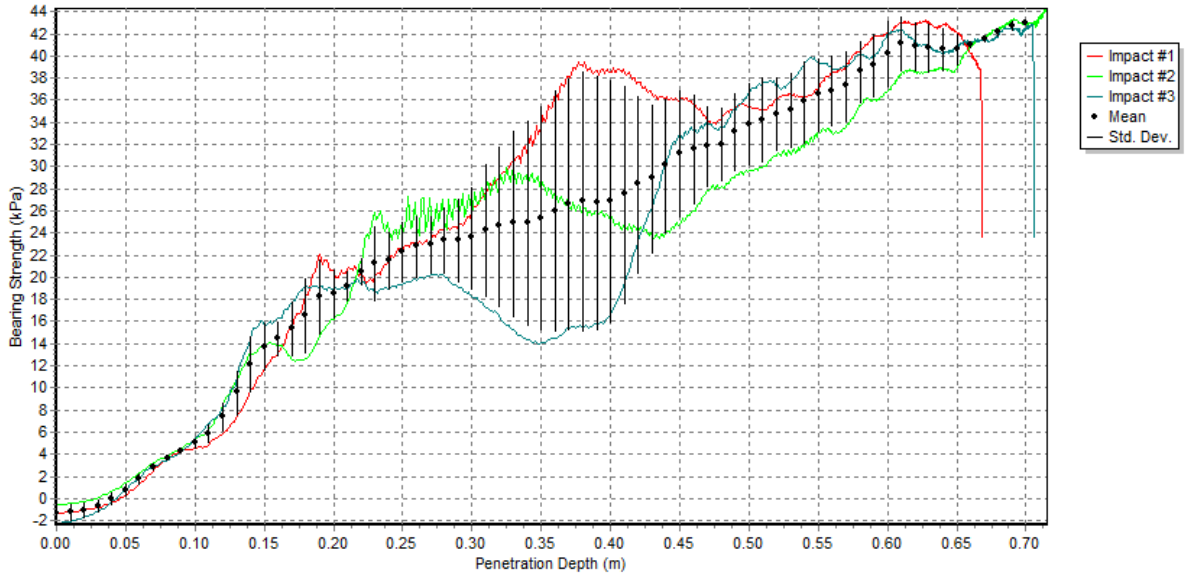

Station 14:

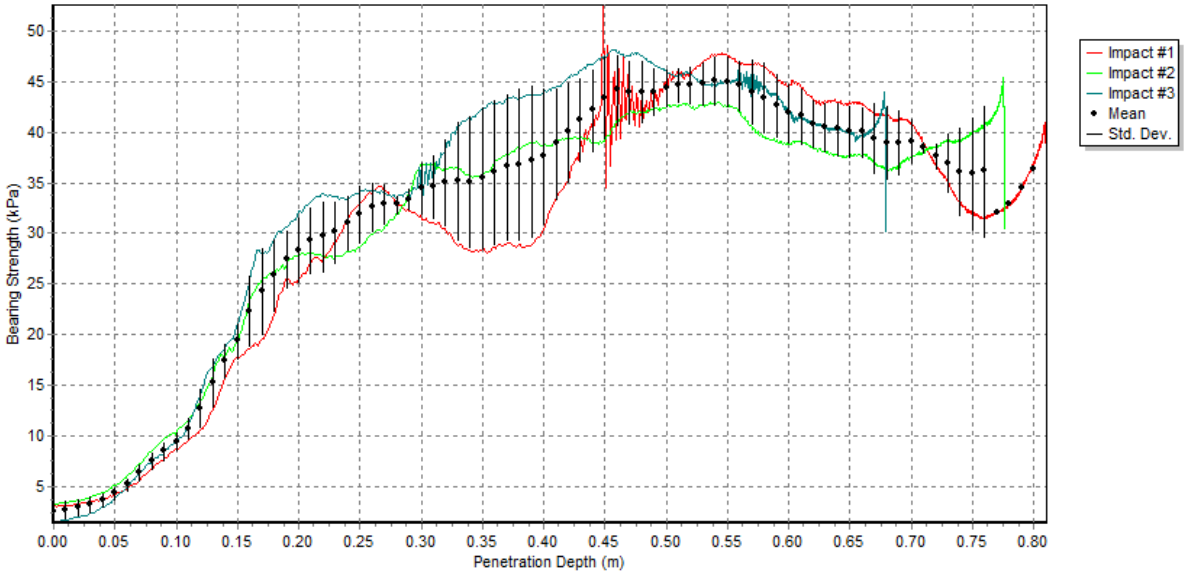


Station 15:

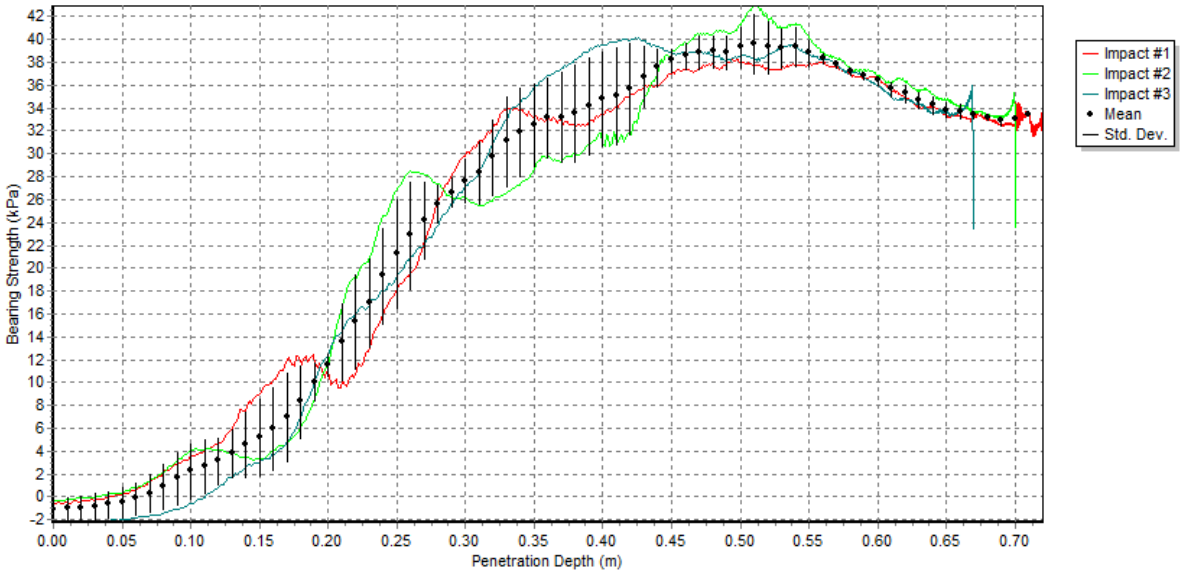

Station 16:

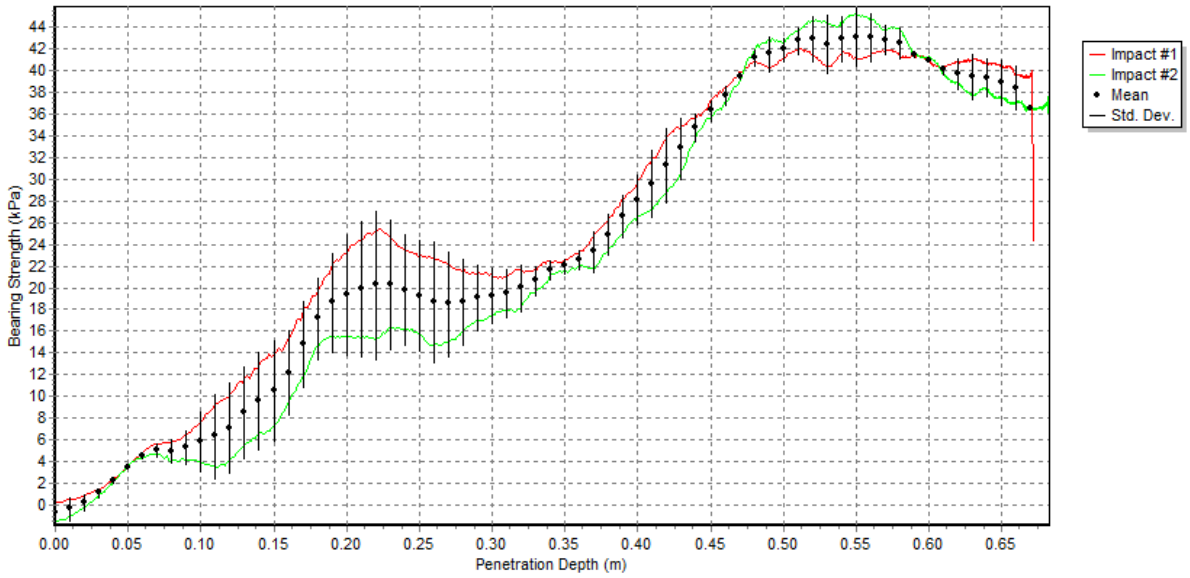


Station 17:

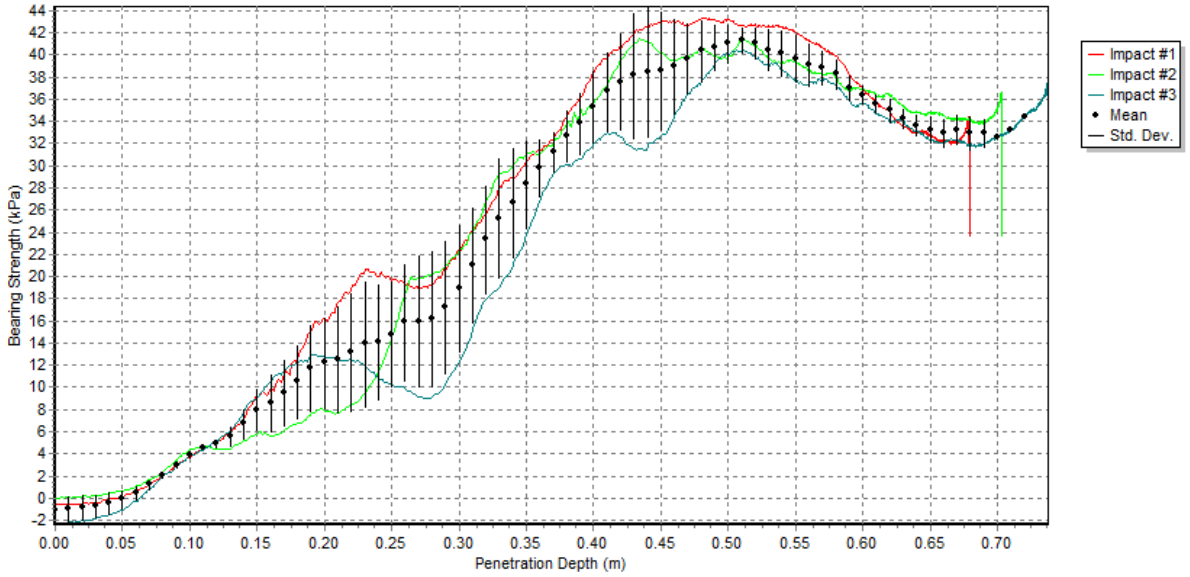

Station 18:

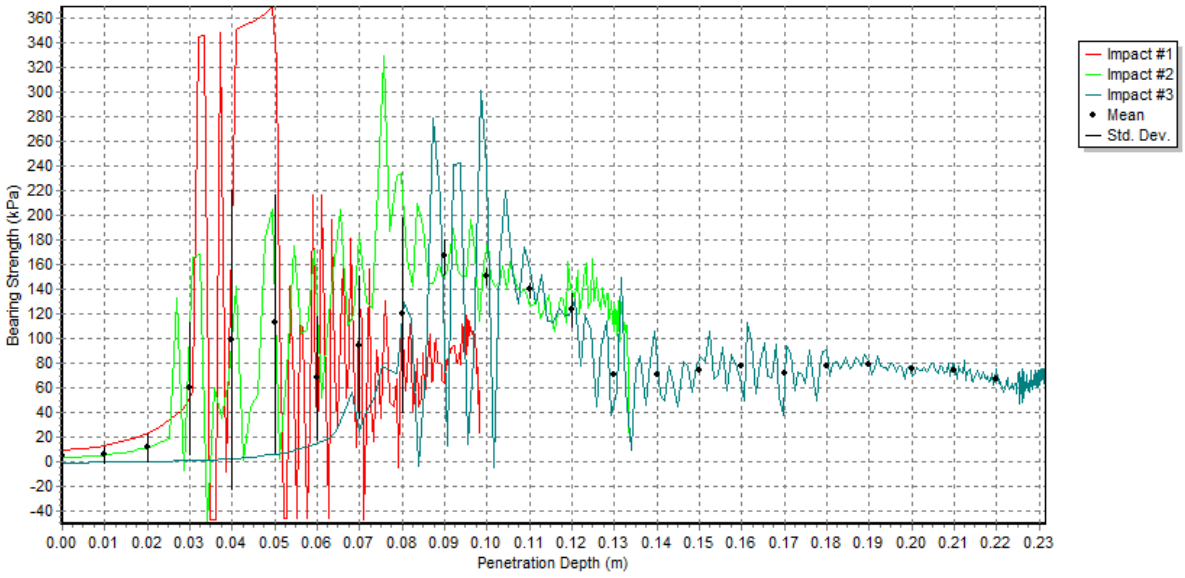


Station 19:

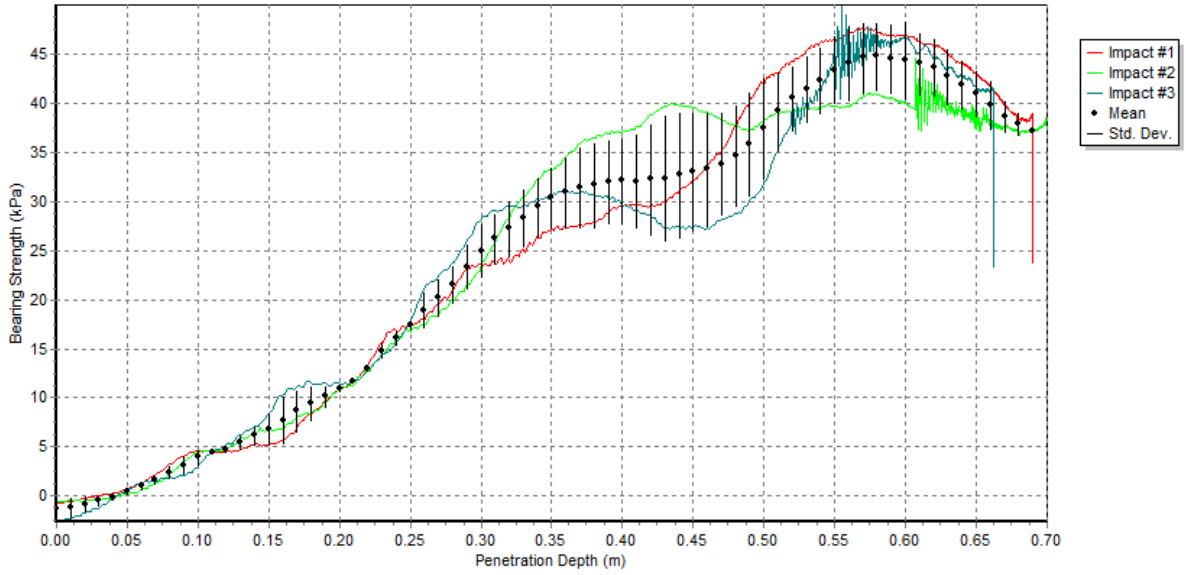

Station 20:

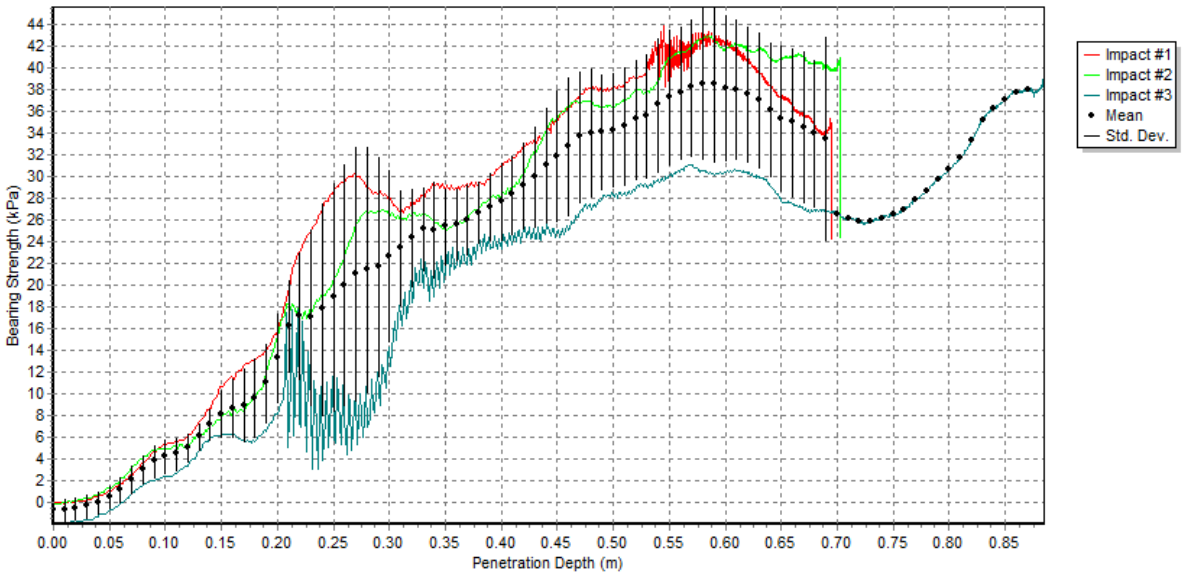


Station 21:

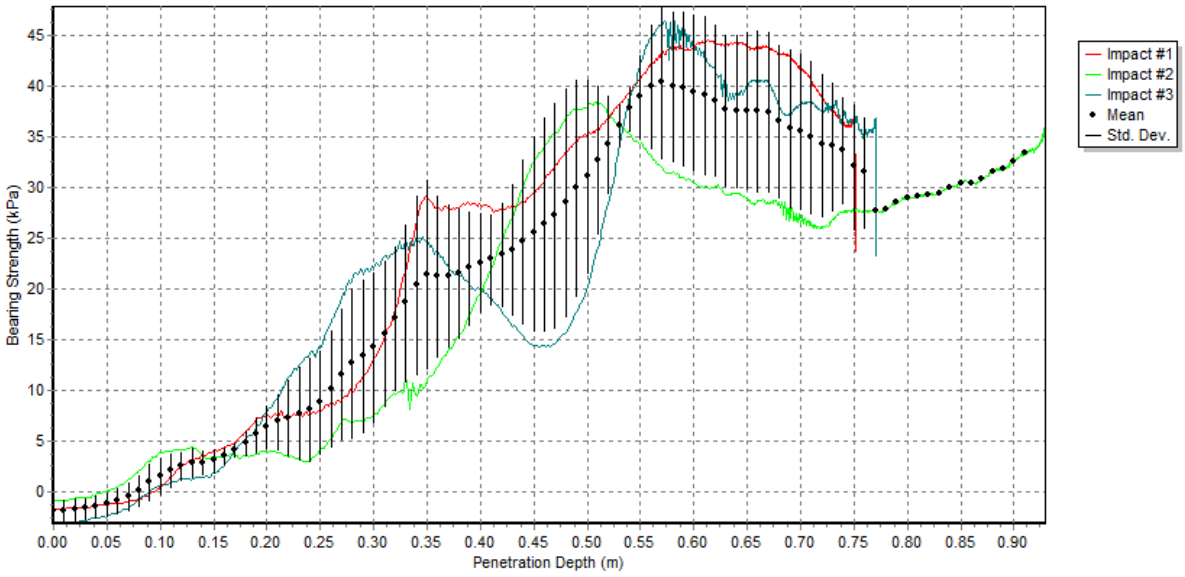

Station 22:

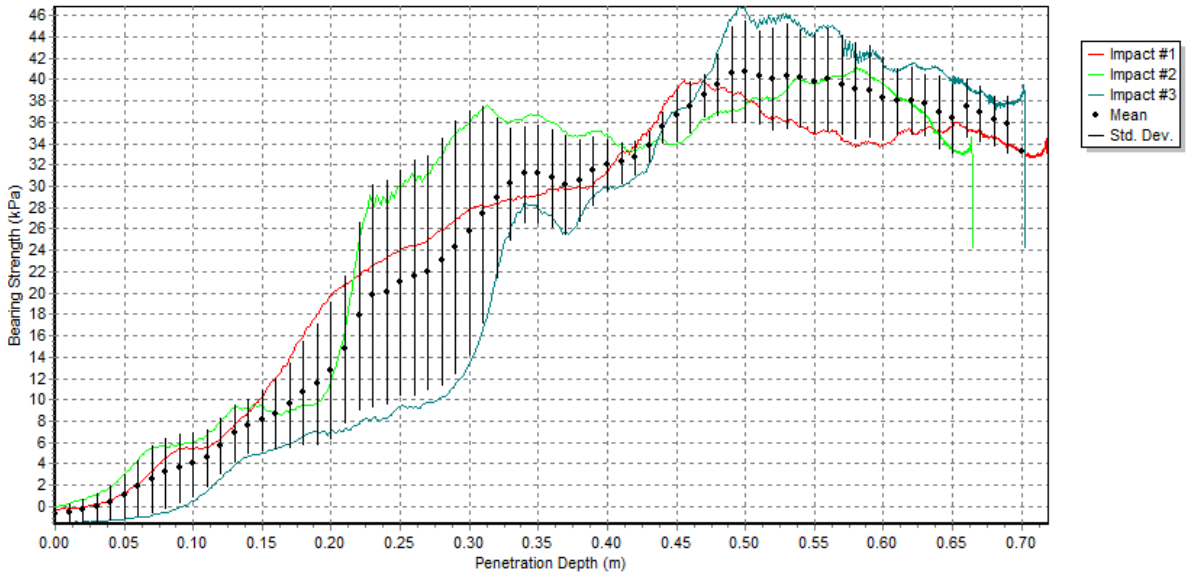


Station 23:

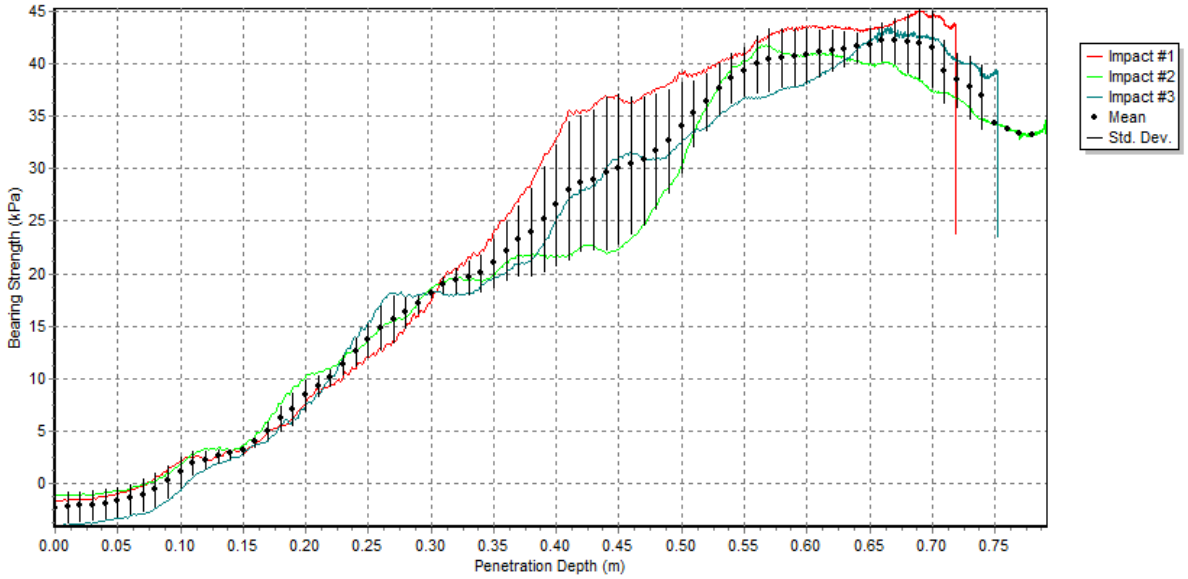

Station 24:

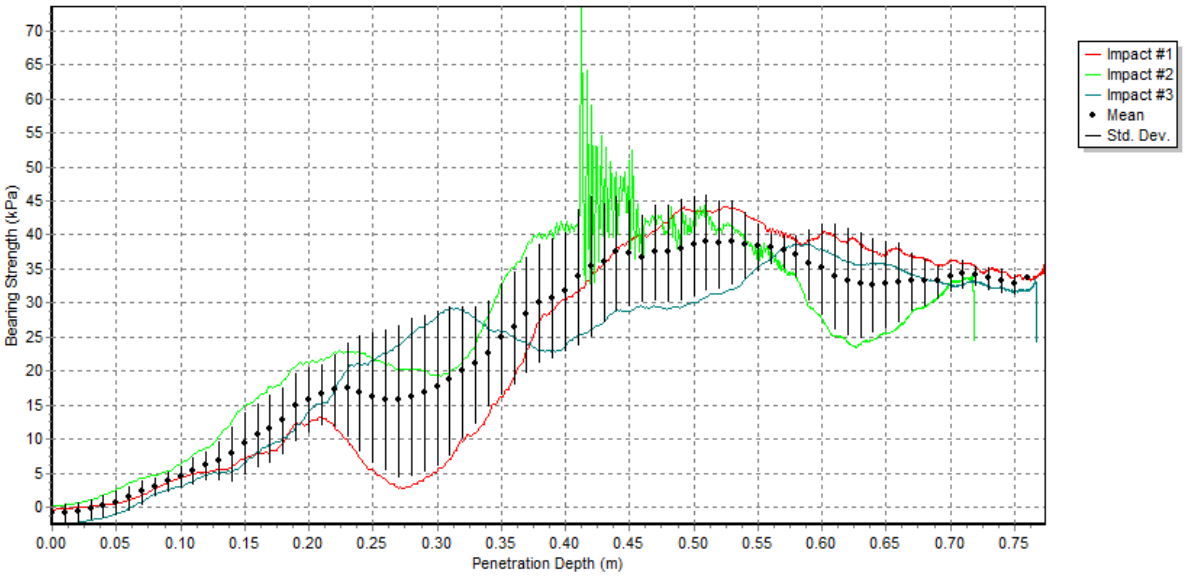


Station 25:

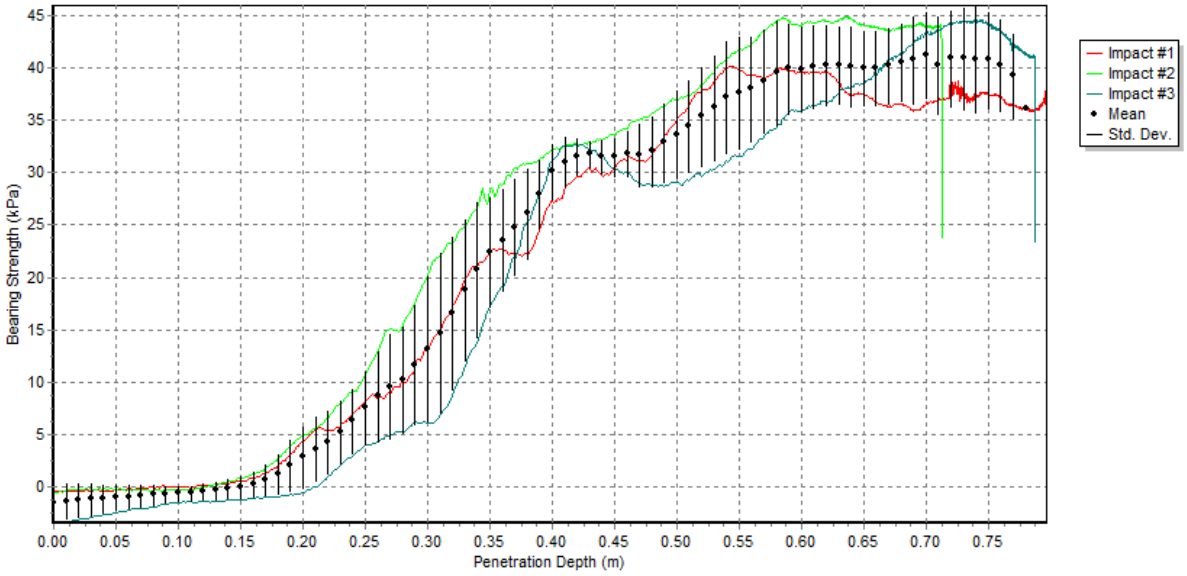

Station 26:

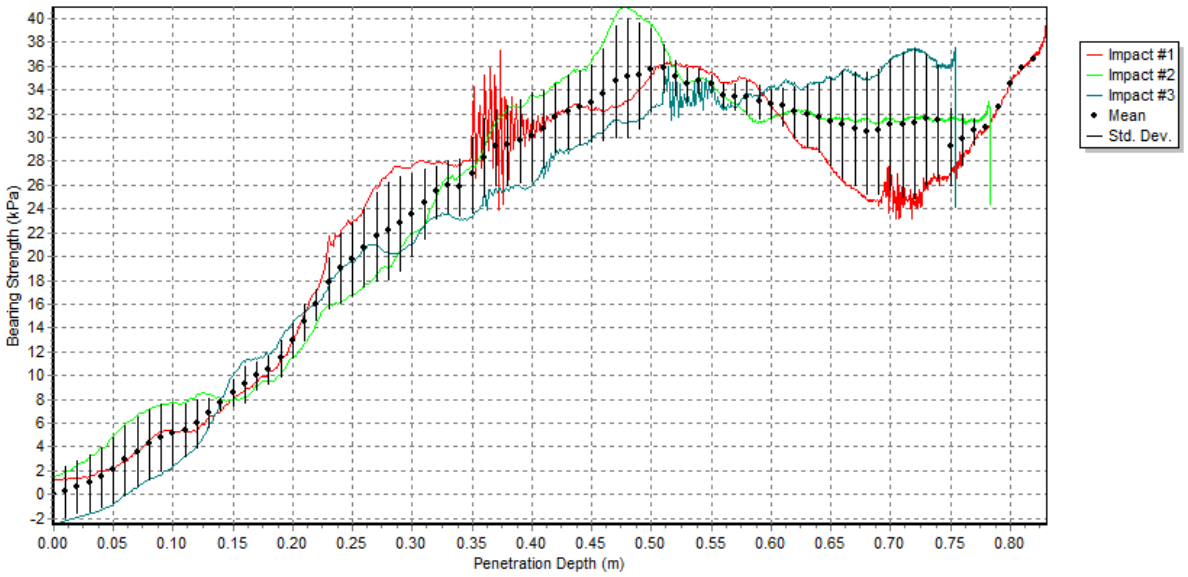


Station 29:

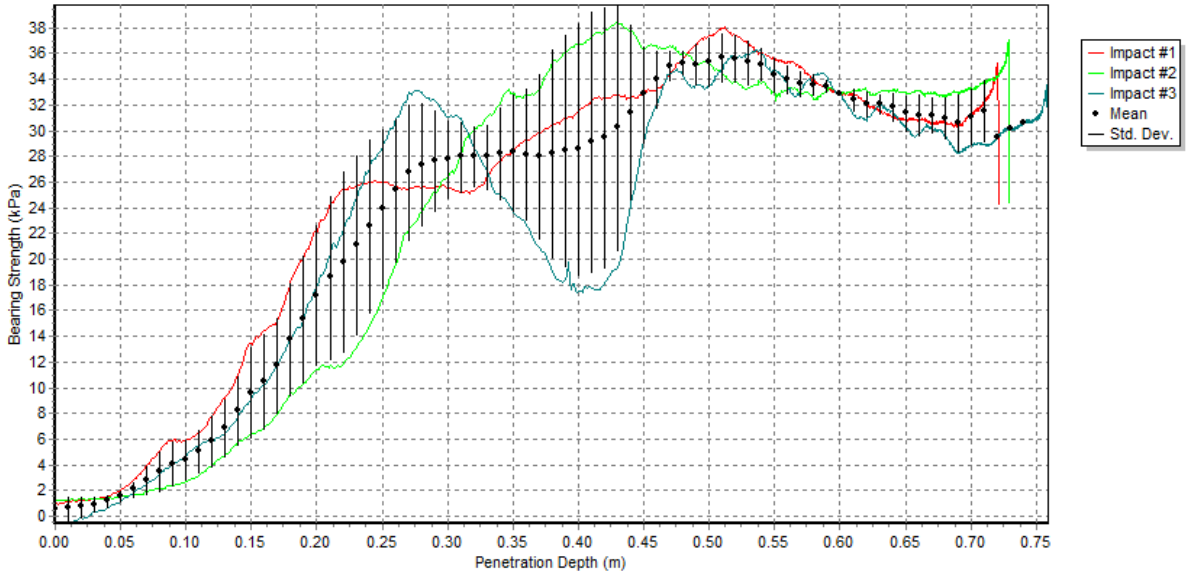

Station 30:

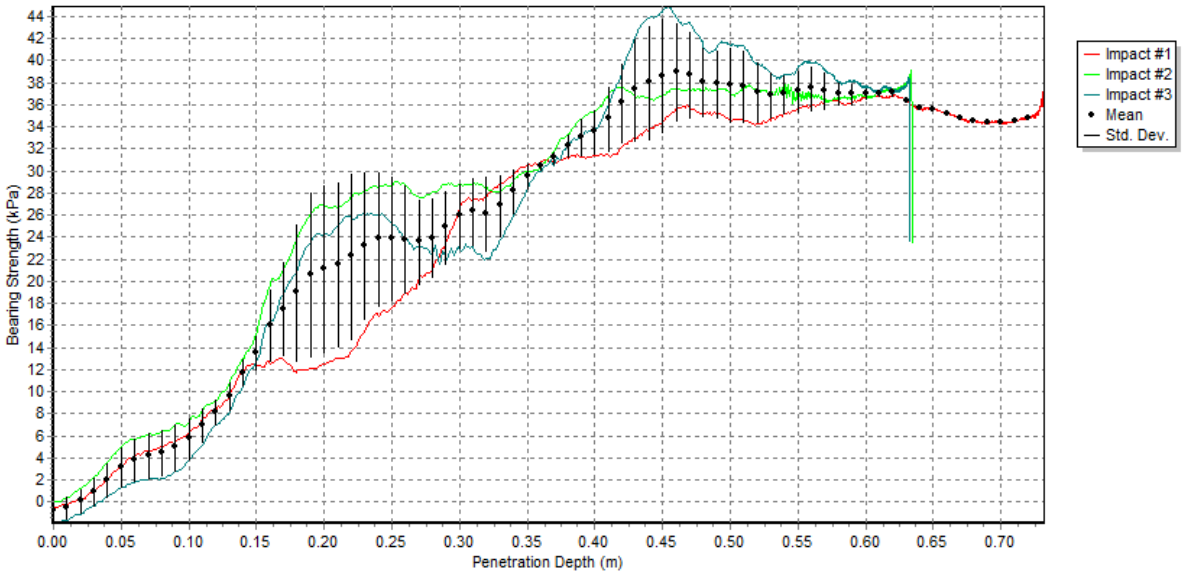


Station 32:

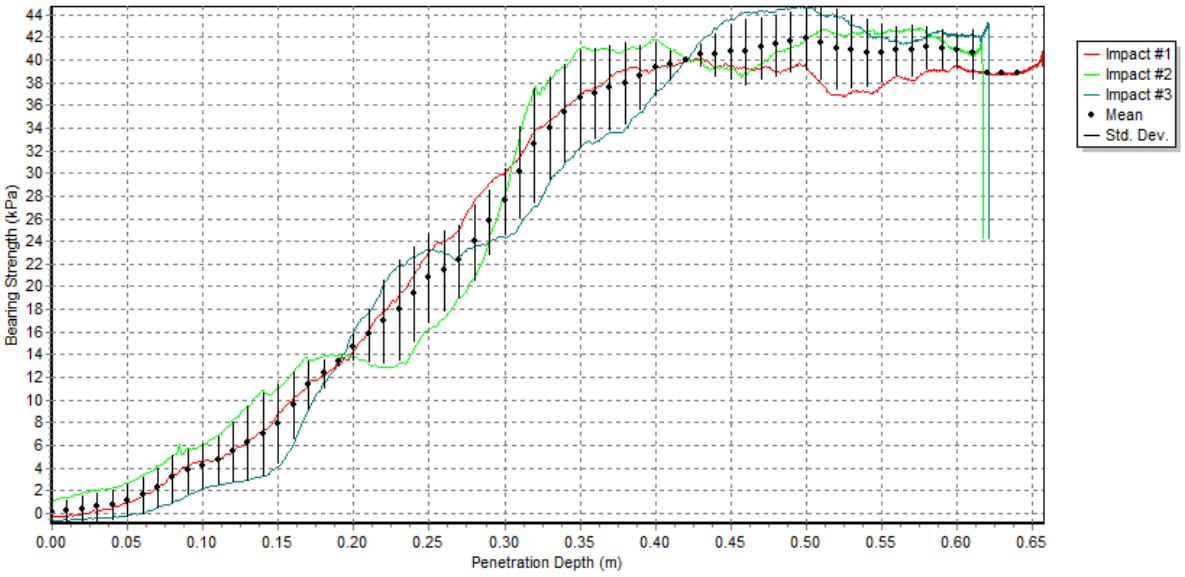

Station 33:

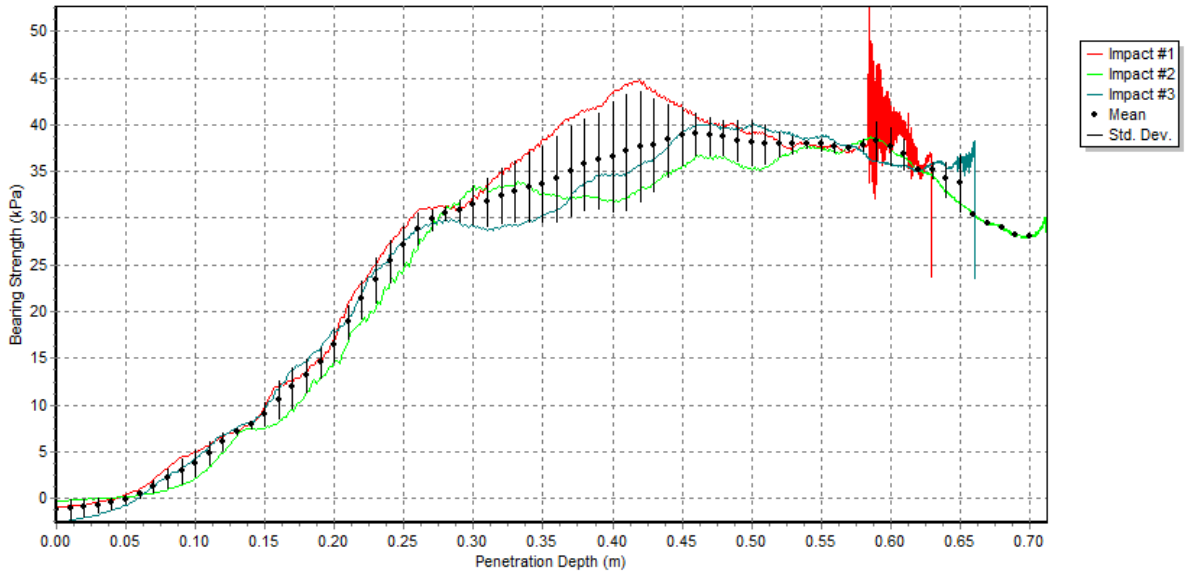


Station 34:

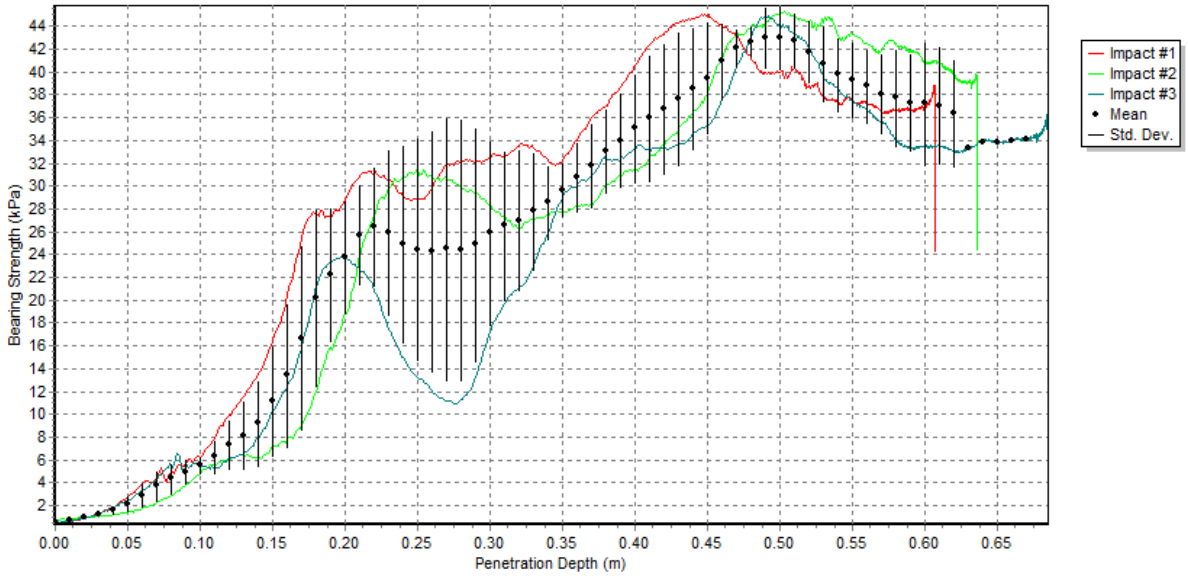

Station 35:

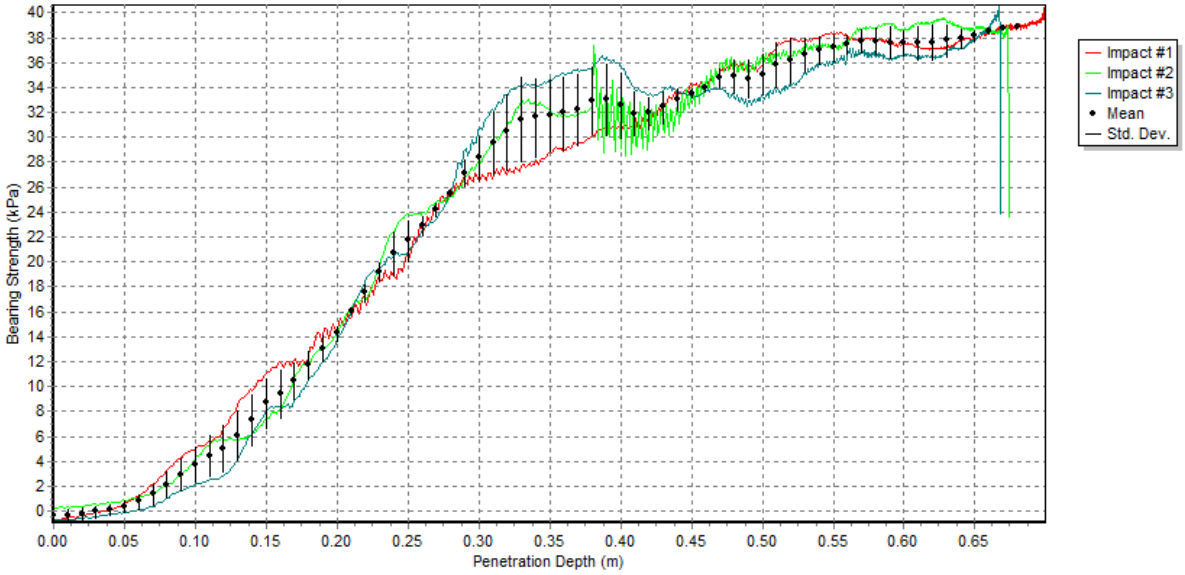


Station 36:

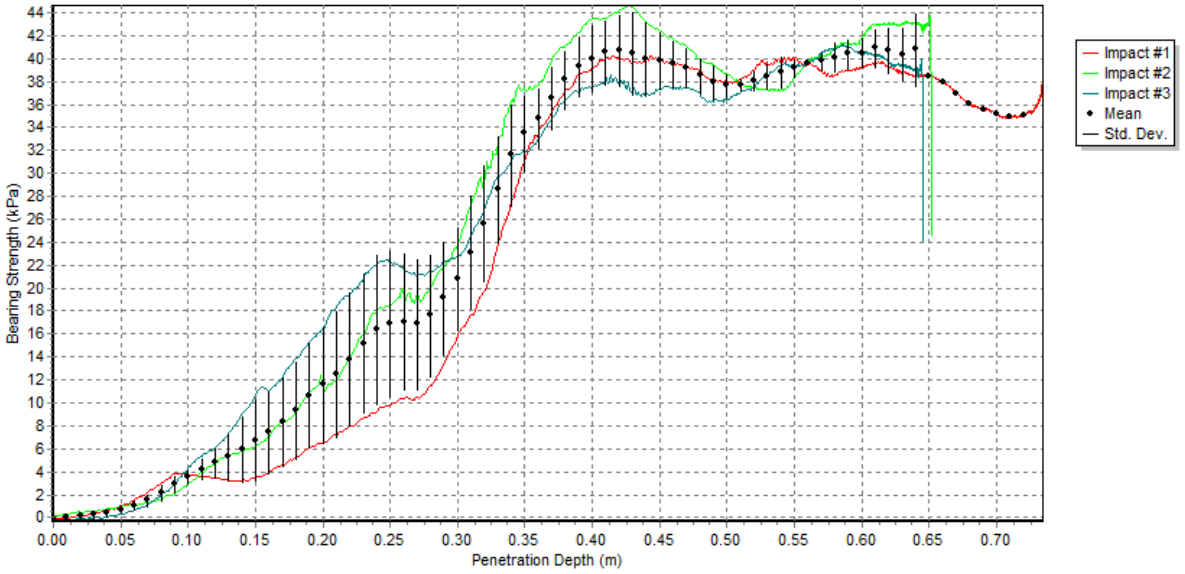

Station 37:

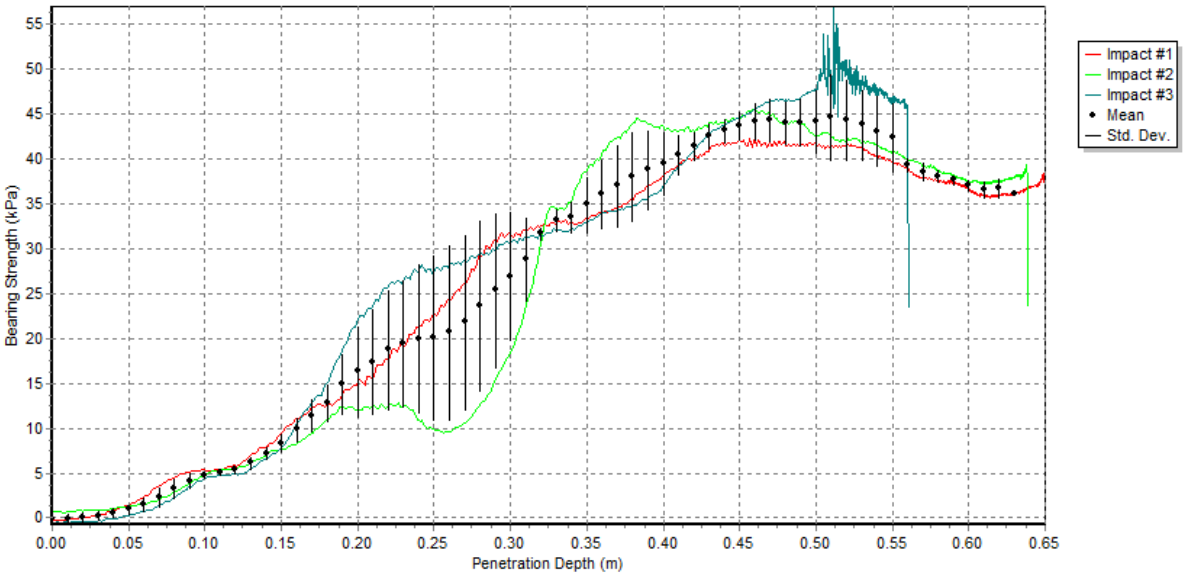


Station 38:

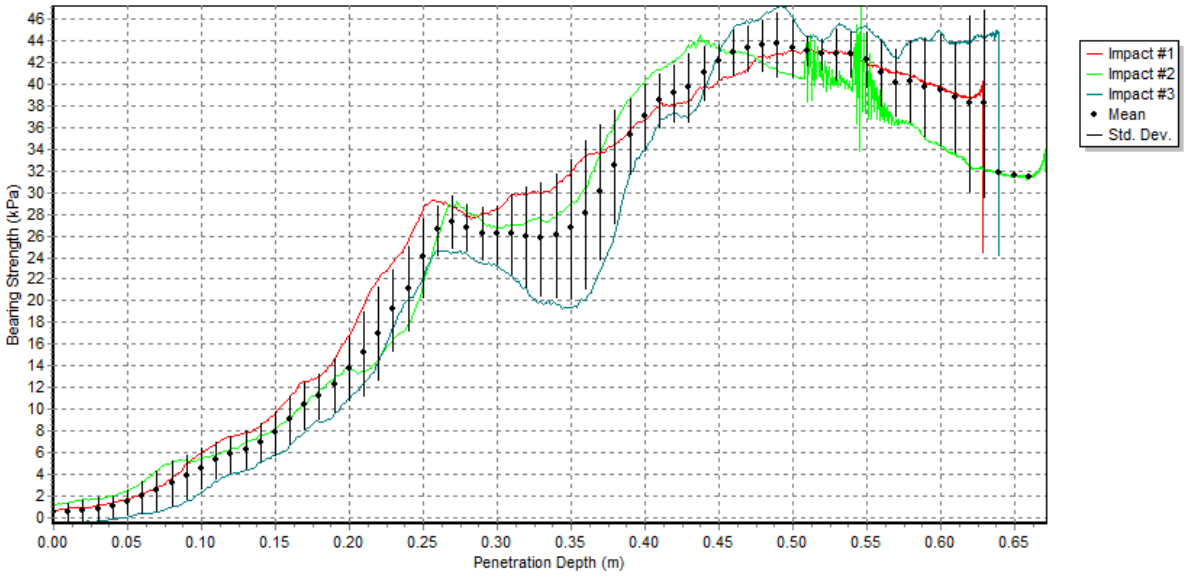

Station 39:

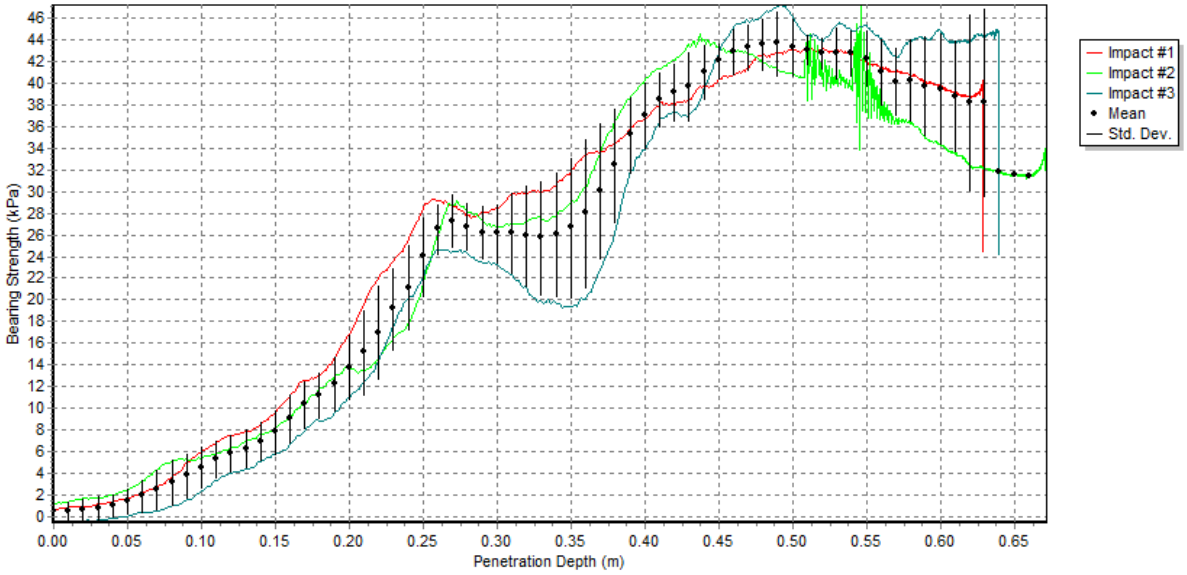


Station 42:

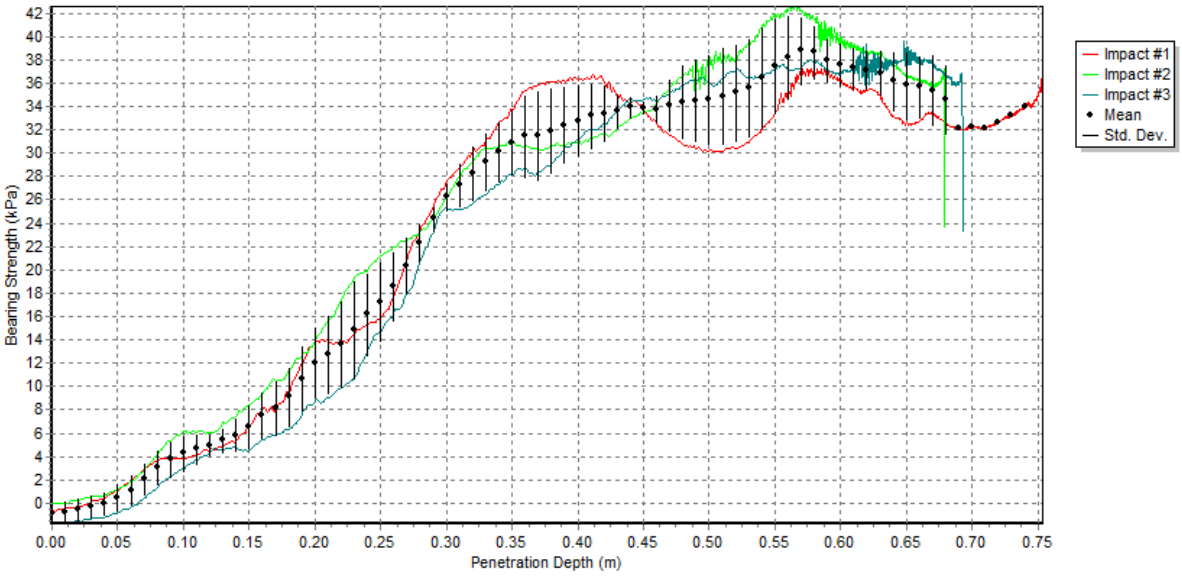

Station 45:

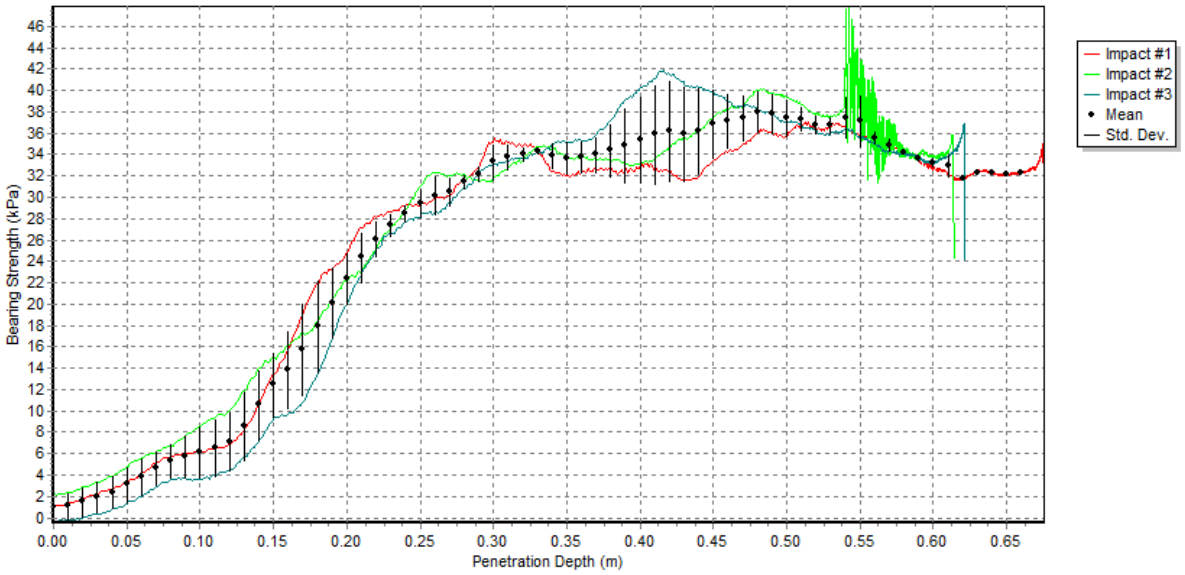


Station 48: